

## Supporting Information

### **A mitochondria-localized iridium(III) photosensitizer for two-photon photodynamic immunotherapy against melanoma**

Lili Wang,<sup>a,e</sup> Johannes Karges,<sup>b</sup> Fangmian Wei,<sup>a</sup> Lina Xie,<sup>a</sup> Zhuoli Chen,<sup>a</sup> Gilles Gasser,<sup>\*c</sup> Liangnian Ji,<sup>a</sup> and Hui Chao<sup>\*a,d</sup>

<sup>a</sup> MOE Key Laboratory of Bioinorganic and Synthetic Chemistry, School of Chemistry, Guangdong Provincial Key Laboratory of Digestive Cancer Research, The Seventh Affiliated Hospital, Sun Yat-Sen University, Guangzhou, 510006, P. R. China.

<sup>b</sup> Faculty of Chemistry and Biochemistry, Ruhr-University Bochum, Universitätsstrasse 150, 44780 Bochum, Germany.

<sup>c</sup> Chimie ParisTech, PSL University, CNRS, Institute of Chemistry for Life and Health Sciences, Laboratory for Inorganic Chemical Biology, Paris, 75005, France.

<sup>d</sup> MOE Key Laboratory of Theoretical Organic Chemistry and Functional Molecule, School of Chemistry and Chemical Engineering, Hunan University of Science and Technology, Xiangtan, 400201, P. R. China.

<sup>e</sup> Public Research Center, Hainan Medical University, Haikou, 571199, P. R. China.

E-mail: ceschh@mail.sysu.edu.cn; gilles.gasser@chimieparistech.psl.eu.

# Contents

## Supplementary Methods

### Supplementary Notes

**Scheme S1.** The synthetic route of Ir-pbt-Bpa.

**Fig. S1**  $^1\text{H}$  NMR spectrum and ESI-MS spectra of Ir-pbt-Bpa in  $\text{CH}_3\text{OH}$ .

**Fig. S2** The purity of Ir-pbt-Bpa by HPLC.

**Fig. S3** The photophysical properties of Ir-pbt-Bpa.

**Fig. S4** Two-photon absorption cross-section spectra of Ir-Bpa and Ir-pbt-Bpa.

**Fig. S5** Assessment of the photostability of Ir-Bpa and Ir-pbt-Bpa by ESI-MS.

**Fig. S6** Assessment of the photostability of Ir-Bpa and Ir-pbt-Bpa by  $^1\text{H}$  NMR.

**Fig. S7** HPLC analysis of Ir-pbt-Bpa incubated in FBS for 0 h or 48 h.

**Fig. S8** Determination of the singlet oxygen quantum yield of Ir-Bpa and Ir-pbt-Bpa.

**Fig. S9** Electron spin resonance spectrum of Ir-Bpa and Ir-pbt-Bpa with  $^1\text{O}_2$ .

**Fig. S10** Electron spin resonance spectrum of Ir-Bpa and Ir-pbt-Bpa with  $\bullet\text{O}_2^-$ .

**Fig. S11** Fluorescent images of B16F10 cells co-stained by calcein-AM and propidium iodide with Ir-pbt-Bpa.

**Fig. S12** Log P values of complexes Ir-Bpa and Ir-pbt-Bpa.

**Fig. S13** Flow cytometry spectrum upon treatment of B16F10 cells with Ir-pbt-Bpa to investigate the ability of the compound to generate ROS.

**Fig. S14** Flow cytometry spectrum upon treatment of B16F10 cells with Ir-pbt-Bpa to investigate the ability of the compound to generate LPO with Ir-pbt-Bpa upon irradiation (750 nm).

**Fig. S15** Representative immunoblotting images of the Western Blot of B16F10 cells upon treatment with Ir-pbt-Bpa for p-eIF and CHOP.

**Fig. S16** Flow cytometry spectrum upon treatment of B16F10 cells with Ir-pbt-Bpa to investigate the ability of the compound to release  $\text{Ca}^{2+}$  ions.

**Fig. S17** Relative glutathione-disulfide/glutathione ratio upon treatment of A375 cells with Ir-pbt-Bpa.

**Fig. S18** Representative immunoblotting images of the Western Blot of A375 cells upon treatment with Ir-pbt-Bpa for GPX4.

**Fig. S19** Flow cytometry spectrum upon treatment of B16F10 cells with Ir-pbt-Bpa to investigate the ability of the compound to generate LPO.

**Fig. S20** Confocal laser scanning microscopy images of A375 cells upon incubation with Ir-pbt-Bpa for LPO.

**Fig. S21** Confocal laser scanning microscopy images of B16F10 cells upon incubation with Ir-pbt-Bpa for LPO.

**Fig. S22** Fluorescence microscopy images of LPO of A375 cells upon treatment with Ir-pbt-Bpa upon irradiation (750 nm).

**Fig. S23** Cell viability of A375 cells upon pre-incubation with the cell death inhibitors and treated with Ir-pbt-Bpa.

**Fig. S24** Immunofluorescence confocal laser scanning microscopy upon treatment of A375 cells with Ir-pbt-Bpa for HSP70.

**Fig. S25** Release of HMGB1 protein upon treatment of A375 cells with Ir-pbt-Bpa under different illumination powers.

**Fig. S26** Release of ATP upon treatment of A375 cells with Ir-pbt-Bpa under different illumination powers.

**Fig. S27** Immunofluorescence confocal laser scanning microscopy upon treatment of B16F10 cells with Ir-Bpa and Ir-pbt-Bpa for calreticulin.

**Fig. S28** Immunofluorescence confocal laser scanning microscopy upon treatment of B16F10 cells with Ir-Bpa and Ir-pbt-Bpa for HMGB1.

**Fig. S29** Flow cytometry spectrum to investigate the translocation of calreticulin upon treatment of B16F10 cells with Ir-Bpa and Ir-pbt-Bpa.

**Fig. S30** Release of HMGB1 upon treatment of B16F10 cells with Ir-Bpa and Ir-pbt-Bpa.

**Fig. S31** Release of ATP upon treatment of B16F10 cells with Ir-Bpa and Ir-pbt-Bpa.

**Fig. S32** Fluorescence microscopy images of A375 MCTS co-stained by propidium iodide with Ir-pbt-Bpa.

**Fig. S33** Histological examination of the main organs of the mice on day 12.

**Fig. S34** Representative flow cytometry plots indicate the proportions of dendritic cells in lymph nodes on day 7.

**Fig. S35** Representative flow cytometry plots indicate the proportions of CD8<sup>+</sup> T cells in tumors on day 12.

**Fig. S36** Representative flow cytometry plots indicate the proportions of regulatory T cells in tumors on day 12.

**Fig. S37** Immunofluorescence confocal laser scanning microscopy stained with CD8<sup>+</sup> and Foxp3<sup>+</sup> specific antibodies in secondary tumor slices on day 12.

**Fig. S38** Representative flow cytometry plots indicate the proportions of effector memory T cells in tumors on day 12.

**Fig. S39** Representative flow cytometry plots indicate the proportions of CD8<sup>+</sup> T cells in the spleen on day 12.

**Fig. S40** Representative flow cytometry plots indicate the proportions of regulatory T cells in spleens on day 12.

**Fig. S41** Representative flow cytometry plots indicate the proportions of effector memory T cells in the spleen on day 12.

**Table S1.** 48 h (photo-)cytotoxicity profile in different cell lines.

**Table S2.** 48 h (Photo)cytotoxicity profile under various light conditions towards A375 cells.

**Table S3.** 48 h (Photo)cytotoxicity of Ir-pbt-Bpa towards A375 MCTS.

## Supplementary Methods

**Materials.**  $[\text{Ir}(\text{pbt})_2\text{Cl}]_2$ <sup>1</sup> and N-([2,2'-bipyridin]-4-yl)-4-phenylbutanamide (Bpa)<sup>2</sup> were synthesized according to a previously reported protocol.<sup>1</sup> All reagents were commercially available and used without further purification unless specifically noted.  $\text{IrCl}_3 \cdot x\text{H}_2\text{O}$ , 4-Phenylbutyric acid, 2-phenylbenzo[d] thiazole (pbt), 2-(Benzo[b]thiophen-2-yl)pyridine, 2-(1H-Benzotriazole-1-yl)-1,1,3,3-tetramethyluronium hexafluorophosphate (HBtU), Ethyldiisopropylamine (DIPEA), 4-dimethylaminopyridine (DMAP) were obtained from Energy Chemical (China). 3-(4,5-dimethylthiazol-2-yl)-2,5-diphenyltetrazolium bromide (MTT) were purchased from MP Biomedicals (USA). Calreticulin (D3E6) XP<sup>®</sup> Rabbit mAb, HMGB1 Antibody, Anti-rabbit IgG (H+L), F(ab')<sub>2</sub> Fragment (Alexa Fluor<sup>®</sup> 647 Conjugate), Anti-rabbit IgG (H+L), F(ab')<sub>2</sub> Fragment (Alexa Fluor<sup>®</sup> 555 Conjugate), Phospho-eIF2 $\alpha$  (Ser51) Antibody, and eIF2 $\alpha$  (D7D3) XP<sup>®</sup> Rabbit mAb were purchased from Cell Signaling Technology (USA). Tubulin- $\alpha$  polyclonal antibody was obtained from Bioworld Technology. Anti-Hsp70 mAb, Anti-DDIT3 (CHOP) Ab, and Anti-Glutathione Peroxidase 4 antibody was purchased from Abcam (USA). Fluo-4 AM and GSH and GSSG Assay Kit was purchased from Beyotime Biotechnology (China). MitoTracker<sup>™</sup> Red and the 2', 7'-dichlorofluorescein diacetate (DCFH-DA) kit were purchased from Thermo Scientific (USA). Image-iT<sup>®</sup> Lipid Peroxidation Kit, Nucleoprotein Extraction Kit, Cytoplasmic and Mitochondrial Protein Extraction Kit were bought from Life Technology. Endoplasmic Reticulum Isolation Kit was purchased from Sigma-Aldrich (USA). ENLITEN<sup>®</sup> ATP Assay System Bioluminescence Detection Kit and CellTiter-Glo<sup>®</sup> 3D Cell Viability Kit was purchased from Promega (USA). HMGB1 Detection Kit was purchased from Chondrex (USA). Dulbecco's modified eagle medium (DMEM), fetal bovine serum (FBS), and penicillin-streptomycin were obtained from Gibco (USA).

**Instruments.** Electrospray mass spectra (ES-MS) were detected on an LCQ system (Finnigan MAT, USA). <sup>1</sup>H NMR spectra were performed on a nuclear magnetic resonance spectrometer (Bruker Avance III, 400 MHz), All chemical shifts are given relative to tetramethylsilane (TMS). UV-Vis spectra were recorded on a Perkin-Elmer Lambda 850 spectrophotometer. Emission spectra were recorded by a Perkin-Elmer LS 55 spectrofluorophotometer at room temperature. The two-photon absorption (TPA) cross-section was measured with Femtosecond Fluorescence Spectrum Measurement System (Coherent Inc, USA). Electron spin resonance spectroscopy (ESR) spectra were measured using a Bruker e-scan ESR spectrometer. ATP experiments were recorded on TECAN Infinite M200 PRO multifunctional reader. ICP-MS were recorded on an iCAP RQ (Thermo Fisher) spectrometer. Instruments for Western blot experiments are from Bio-Rad. Confocal cell imaging and the imaging of fluorescently stained sections of tumors and spleens were conducted on LSM 880 (Carl Zeiss, Germany) Laser Scanning Confocal Microscope with two-photon laser. The H&E stained sections were observed with a Carl Zeiss Axio Imager Z2 microscope. Flow cytometry

experiments were conducted on BD FACS Canto II. Two-photon irradiation in animal vaccine experiments was observed with Femtosecond Fluorescence Spectrum Measurement System.

**Synthesis of [Ir(pbt)<sub>2</sub>(Bpa)]Cl (Ir-pbt-Bpa).** [Ir(pbt)<sub>2</sub>Cl]<sub>2</sub> (120 μmol) and Bpa (100 μmol) were dissolved in a mixture of methanol and chloroform (1:1, 20 mL) and heated at 65°C for 6 h under argon atmosphere. After this time, the solvent was removed under reduced pressure. The crude product was purified by alumina column chromatography using dichloromethane:methanol (10/1, v/v) as an eluent. The fractions containing the product were united and the solvent was removed under reduced pressure. The product was further purified by recrystallization from dichloromethane/toluene. The solid was collected by filtration and washed with diethyl ether. The compound was dried under a vacuum. Yield 40%, m/z = 930.13 ([M-Cl]<sup>+</sup>); <sup>1</sup>H NMR (400 MHz, CD<sub>3</sub>CN) δ 11.82 (s, 1H), 9.23 (d, J = 2.2 Hz, 1H), 8.31 (d, J = 7.7 Hz, 1H), 8.09 (d, J = 7.2 Hz, 3H), 8.01 (dd, J = 7.6, 2.5 Hz, 2H), 7.93 – 7.87 (m, 2H), 7.83 (d, J = 6.3 Hz, 1H), 7.53 – 7.48 (m, 1H), 7.37 (td, J = 8.2, 7.7, 3.9 Hz, 2H), 7.26 – 7.14 (m, 7H), 7.13 – 7.05 (m, 4H), 6.91 – 6.81 (m, 2H), 6.47 (d, J = 8.4 Hz, 1H), 6.42 (d, J = 7.6 Hz, 1H), 6.37 (d, J = 7.6 Hz, 1H), 6.20 (d, J = 8.4 Hz, 1H), 2.65 – 2.59 (m, 2H), 2.55 (t, J = 7.3 Hz, 2H), 2.33 (s, 1H). HPLC purity: t<sub>R</sub> = 11.20, 97.20%.

[Ir(ppy)<sub>2</sub>(Bpa)]Cl (Ir-Bpa) was synthesized according to a previously reported protocol (referred to in the original publication as Ir2).<sup>2</sup>

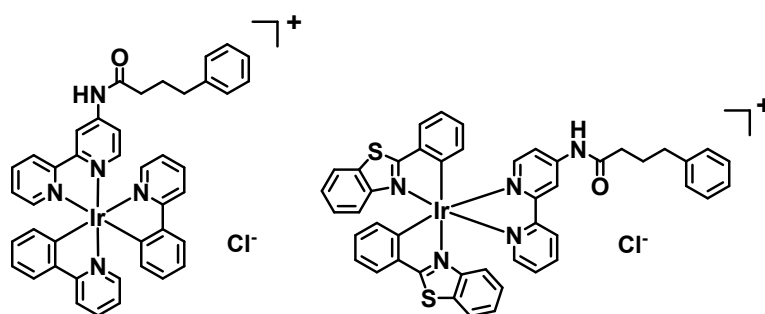


**Chart 1.** Chemical structures of the Ir(III) complexes **Ir-Bpa** (left) and **Ir-pbt-Bpa** (right).

**Two-photon absorption cross-section measurement.** The two-photon absorption (TPA) cross-section was measured according to a previously reported method.<sup>3,4</sup> Samples in methanol (0.1 mM) were placed in a fluorometric quartz cuvette at 37°C. The experimental fluorescence excitation and detection conditions were conducted with negligible reabsorption processes. The TPA spectra were determined from 740-800 nm. And the cross-section value was calculated at each wavelength according to the equation as follows:

$$\delta_2 = \delta_1 \frac{\phi_1 C_1 I_2 n_2}{\phi_2 C_2 I_1 n_1} \quad (1)$$

Where  $\delta$  is the two-photon absorption cross-section,  $\Phi$  is the quantum yield,  $C$  is the concentration,  $I$  is the integrated emission intensity at each wavelength, and  $n$  is the refractive index. Subscript '2' stands for samples, '1' stands for the reference, rhodamine B.

**Electron paramagnetic resonance (EPR) assay.** The type of ROS was identified using the  $^1\text{O}_2$  scavenger 2,2,6,6-tetramethylpiperidine (TEMP) and the superoxide anion radical scavenger 5,5-dimethyl-1-pyrroline N-oxide (DMPO). Solutions of the sample in methanol (100  $\mu\text{M}$ ) were irradiated with a 405 nm LED (0.75 J/cm<sup>2</sup>) light. The ESR signal was recorded using an electron spin resonance spectrometer.

**The stability of Ir(III) complex in FBS solution.** A diazepam (Sigma-Aldrich) solution was used as the internal reference. For this experiment, Ir-pbt-Bpa (5  $\mu\text{M}$ ) and 5  $\mu\text{M}$  diazepam were added to the fetal bovine serum (FBS, 980  $\mu\text{L}$ ) to a total volume of 1000  $\mu\text{L}$ . The solution was incubated for 0 h, or 48 h at 37 °C with shaking (~300 rpm) respectively. 2 mL of acetonitrile was added, and the mixture was centrifuged for 45 min at 1000 g at 4 °C. The supernate was evaporated, and the residue was suspended in 1000  $\mu\text{L}$  of Methanol. The suspension was filtered and analyzed by HPLC–UV. A C8 reverse phase column was used with a flow rate of 1 mL/min. The runs were performed with a linear gradient of A (methyl alcohol, Sigma-Aldrich HPLC grade) in B (distilled water) from 50% to 100% (v/v) in 15 min. Ir-pbt-Bpa (5  $\mu\text{M}$ , from stock solution 1 mM in DMSO) were dissolved in FBS and incubated at 37°C for 0 h, or 48 h, respectively. The absorption spectra of these mixtures were tested.

**Cell lines and culture conditions.** All cells used were obtained from the animal experimental Centre of Sun Yat-Sen University (Guangzhou, China). Cell lines A549, LLC, MDA-MB-231, 4T1, SW620, CT-26, A375, and B16F10 were maintained in DMEM media supplemented with fetal bovine serum (FBS, 10%) at 37 °C in a humidified atmosphere with 5% CO<sub>2</sub>.

**Cell viability assay.** The *in vitro* cytotoxicities of complexes Ir-Bpa and Ir-pbt-Bpa were determined by MTT assay. Briefly, the cells were seeded into 96-well microtiter plates at ( $1 \times 10^4$  cells per well), and grown for 24 h at 37 °C in a 5% CO<sub>2</sub> incubator, before various concentrations of the complexes were added to the culture media. After 4 h incubation, the supernatant was replaced with a fresh culture medium, and cells were subjected to irradiation (405 nm LED, 0.75 J/cm<sup>2</sup>), and incubated for an additional 40 h in the dark. Cells without irradiation were replaced with a fresh culture medium and maintained in the dark. MTT solution (10  $\mu\text{L}$ , 5 mg/mL in 1× PBS) was added to each well. After 4 h of incubation, the cultures were removed and 150  $\mu\text{L}$  of DMSO solution was added

to each well. The optical density of each well was measured on a microplate spectrophotometer at a wavelength of 595 nm. Data were reported as the mean  $\pm$  standard deviation ( $n = 3$ ).

**Cell death mechanism.** The inhibitors were Z-VAD-fmk (10  $\mu$ M), 3-methyladenine (100  $\mu$ M), Ferrostatin-1 (10  $\mu$ M), and Necrostatin-1 (60  $\mu$ M) which were pre-incubated for 30 min.<sup>5</sup> Then Ir-pbt-Bpa (1  $\mu$ M, 2  $\mu$ M) was directly incubated for 4 h, respectively. After 4 h incubation, the supernatant was replaced with the corresponding fresh culture medium, and cells were subjected to irradiation (405 nm LED, 0.75 J/cm<sup>2</sup>). Cells without irradiation were replaced with the corresponding fresh culture medium and maintained in the dark. The survival rate of A375 cells was measured by MTT assay after an additional 20 h co-culture with the fresh culture medium with or without the corresponding inhibitors.

**Cellular localization assay.** A375 cells were incubated with Ir-pbt-Bpa (2  $\mu$ M) for 4 h and then co-incubated with Mito Tracker™ Red FM (MTR) for 0.5 h, then washed by PBS three times and visualized by laser confocal microscopy with a 63  $\times$  oil-immersion objective lens immediately. The excitation wavelengths for Ir-pbt-Bpa were 405 nm, while the excitation wavelength of MTR is 561 nm. Emission filter: 580 nm  $\pm$  20 nm for Ir-pbt-Bpa, and 640  $\pm$  20 nm for MTR. For ICP-MS study, exponentially growing A375 cells were treated with Ir-pbt-Bpa (2  $\mu$ M) at 37 °C for 4 h, respectively. After incubation, the cells were trypsinized, collected, and counted. Each group of cells was divided into three equal portions and treated with Nucleus Extraction Kit, Cytoplasmic and Mitochondrial Protein Extraction Kit, and Endoplasmic Reticulum Isolation Kit according to the manufacturer's protocol. The extract was digested with 60% HNO<sub>3</sub> for more than 2 days and diluted with water to obtain 2% HNO<sub>3</sub> sample solution for final determination. The content of Ir was determined by the standard curve method, and the relationship between the contents of the nucleus, cytoplasm, mitochondria, and ER and the number of cells was calculated. The Ir content was measured by inductively coupled plasma mass spectrometry (ICP-MS).

**Intracellular ROS level detection.** As a probe for ROS generation, non-fluorescent DCFH-DA can be converted to fluorescent 2,7-dichlorodihydrofluorescein (DCFH), which remains in cells. The cells were incubated on a six-well plate with the sample for 4 h at 37°C in dark. The cells were further incubated with 2',7'-dichlorofluorescein diacetate for an additional 30 min. The sample was irradiated with light at 405 nm LED (0.75 J/cm<sup>2</sup>). After light irradiation, the cells were instantly collected and washed twice with PBS. The cell pellets from the six-well plates were resuspended in 500  $\mu$ L of PBS and then examined using the flow cytometer. Six sets of treatments were performed: Control (I): Cells were in the dark; light only (II): Cells were incubated 4 h later and were exposed to irradiation (405 nm LED, 0.75 J/cm<sup>2</sup>); Ir-pbt-Bpa only (III/V): Cells were incubated

with Ir-pbt-Bpa for 4 h (Concentrations:  $IC_{50}/2 \times IC_{50}$ ); Ir-pbt-Bpa + light (IV/VI): Cells were incubated with Ir-pbt-Bpa for 4 h (Concentrations:  $IC_{50}/2 \times IC_{50}$ ) and exposed to irradiation (405 nm LED, 0.75 J/cm<sup>2</sup>).

**Intracellular ROS levels detection upon two-photon irradiation.** A375 cells were incubated with Ir-pbt-Bpa (2.5  $\mu$ M) for 4 h and then co-incubated with corresponding dye for 0.5 h, then washed with PBS three times. The sample was irradiated with light at 750 nm laser (50 mW/cm<sup>2</sup>, 30 s). And visualized by laser confocal microscopy with a 63  $\times$  oil-immersion objective lens before and after two-photon ( $\lambda_{ex} = 750$  nm) irradiation. The excitation wavelength for the dye was 488 nm. Emission filter: 525nm  $\pm$  25 nm for 2,7-dichlorodihydrofluorescein (DCFH).

**Lipid peroxidation.** The generation of lipid peroxidation was investigated using the image-iT<sup>®</sup> Lipid Peroxidation Kit. The cells were incubated on 6-well plates. And divided into six groups. The sample was added to the relevant wells and incubated for 4 h in the dark. Six sets of treatments were performed: Control (I): Cells were kept in the dark; light only (II): Cells were incubated 4 h later and were exposed to irradiation (405 nm LED, 0.75 J/cm<sup>2</sup>); Ir-pbt-Bpa only (III/V): Cells were incubated with Ir-pbt-Bpa for 4 h (Concentration:  $IC_{50}/2 \times IC_{50}$ ); Ir-pbt-Bpa + light (IV/VI): Cells were incubated with Ir-pbt-Bpa for 4 h (Concentration:  $IC_{50}/2 \times IC_{50}$ ) and exposed to irradiation (405 nm LED, 0.75 J/cm<sup>2</sup>). Flow cytometry was used to detect the cells after corresponding treatments.

**Intracellular GSH level detection.** GSH detection was investigated in A375 cells by using GSH and GSSG assay kits. A375 cells were incubated on a six-well plate with the sample for 4 h at 37  $^{\circ}$ C in the dark. The supernatant was replaced with a fresh culture medium and cells were subjected to irradiation (405 nm LED, 0.75 J/cm<sup>2</sup>). Cells without irradiation were replaced with a fresh culture medium and maintained in the dark. After 1 h of the additional incubation, the cells were collected and washed twice with PBS. Then the manufacturer's protocol was followed.

**Immunofluorescence staining of calreticulin in cells.** Confocal laser scanning microscopy: After co-incubation with the drugs for 4 h, the supernatant of all samples was replaced with the fresh culture medium before irradiation. Cells were incubated for an additional 20 h. The cells were stained with Calreticulin (D3E6) XP<sup>®</sup> Rabbit mAb and Anti-Rabbit IgG (H+L), F(ab')<sub>2</sub> Fragment (Alexa Fluor<sup>®</sup> 647 Conjugate), and then Hoechst for 15 min after being washed with PBS. After washing in PBS again, the slides were imaged using the confocal microscope. The excitation wavelength was 633 nm. Emission was collected at 690  $\pm$  40 nm. Flow cytometry: The dosing treatment in this experiment is consistent with the confocal experiment. After light irradiation, the cells were digested with trypsin, fixed by 4% paraformaldehyde, then stained with Calreticulin (D3E6) XP<sup>®</sup>



Rabbit mAb and Anti-Rabbit IgG (H+L), F(ab')<sub>2</sub> Fragment (Alexa Fluor® 647 Conjugate) according to the manufacturer's instructions.

**Immunofluorescence staining of calreticulin in MCTS.** Four sets of treatments were performed on A375 MCTS: 1) The MCTS were incubated in the dark; 2) The MCTS were incubated for 12 h and were exposed to irradiation (750 nm laser, 50 mW, 5 min); 3) The MCTS were incubated with Ir-pbt-Bpa (5 μM) in A375 for 12 h; 4) The MCTS were incubated with Ir-pbt-Bpa (5 μM) in A375 for 12 h and exposed to irradiation (750 nm laser, 50 mW, 5 min). A375 MCTS were incubated for an additional 36 h. The Calreticulin expression of multi-step treated MCTS was tested by confocal microscopy.

**Immunofluorescence staining of extracellular HMGB1 in cells.** The cells were treated in the same way as for the experiment on Calreticulin. The extracellular HMGB1 in cells were stained with HMGB1 Antibody and Anti-rabbit IgG (H+L), F(ab')<sub>2</sub> Fragment (Alexa Fluor® 555 Conjugate). The excitation wavelength was 514 nm. Emission was collected at 620 ± 20 nm.

**Extracellular HMGB1 detection assay in cells and MCTS.** The treatment of cells and MCTS was consistent as described in the above experiment of calreticulin. Extracellular release of HMGB1 was performed by using the HMGB1 detection ELISA kit (Chondrex). The supernatant of treated cells and MCTS were transferred to microtubules respectively. The supernatant as samples were centrifuged at 10000 rpm at 4 °C for 3 min. The samples were then transferred to the specific 96-well plate of the HMGB1 Kit. Follow-up experiments were carried out according to the instructions. The relative contents of HMGB1 in each group under each culture condition were expressed by the intensity ratio with the control group and were corrected by cell viability. The data is reported as the mean value ± standard deviation (n = 3).

**Extracellular ATP detection assay in cells and MCTS.** The detection of extracellular ATP was recorded by ATP Bioluminescence Detection Kit (Promega). Upon completion, 100 μL supernatant was mixed with 100 μL Reagents for each assay in opaque-walled plates. The Chemiluminescence Signal of ATP was measured by TECAN Infinite M200 PRO multifunctional reader. The actual values of ATP content in each group were corrected by cell viability under each culture condition. The data were reported as mean ± standard deviation (SD) (n = 3).

**Immunofluorescence staining of HSP70 in A375 cells.** Confocal laser scanning microscopy: After co-incubation with Ir-pbt-Bpa (1 μM) for 4 h, the supernatant of all samples was replaced with fresh culture medium before irradiation (405 nm LED, 0.75 J/cm<sup>2</sup>). Cells were incubated for an additional 4 h. The cells were stained with Anti-Hsp70 Rabbit mAb and Anti-Rabbit IgG (H+L),

F(ab')<sub>2</sub> Fragment (Alexa Fluor® 647 Conjugate), and then Hoechst for 15 min after being washed with PBS. After washing in PBS again, the slides were imaged using a confocal microscope.

**Western blot analysis.** Western blotting was performed according to the literature description with slight changes. GPX4(17 kDa) Phospho-eIF2 $\alpha$  (38 kDa), eIF2 $\alpha$  (38 kDa), and CHOP (DDIT3, 27 kDa) were detected. Tubulin (52 kDa) was used as the loading control. For GPX4: A375 cells were incubated on 10 cm plates with Ir-pbt-Bpa for 4 h at 37 °C in the dark. The supernatant was replaced with a fresh culture medium and cells were subjected to irradiation (405 nm LED, 0.75 J/cm<sup>2</sup>). Cells without irradiation were replaced with a fresh culture medium and maintained in the dark. After 4 h of the additional incubation, A375 cells were collected and washed twice with PBS. For CHOP, Phospho-eIF2 $\alpha$ , and eIF2 $\alpha$ : Cells were incubated on 10 cm plates with Ir-pbt-Bpa for 4 h at 37 °C in the dark. The supernatant was replaced with a fresh culture medium and cells were subjected to irradiation (405 nm LED, 0.75 J/cm<sup>2</sup>). Cells without irradiation were replaced with a fresh culture medium and maintained in the dark. After 20 h of the additional incubation, A375 cells were collected and washed twice with PBS. Cells were treated on ice with RIPA-Lysis Buffer (Biotime Biotechnology) containing 100  $\mu$ g/mL phenylmethanesulfonyl fluoride (PMSF) for 30 minutes. Cell lysates were centrifuged at 15000 rpm at 4°C for 10 min, and the supernatant was collected and added with SDS-Page Sample Loading Buffer (Biotime Biotechnology). Samples were heated at 100°C for 5 min and then stored at -20°C. Total protein content was determined using the Thermo Scientific™Pierce™BCA protein assay kit to ensure sample consistency. Western Blot was used to detect 20  $\mu$ g protein. PVDF membrane was used to transfer protein (250 mA, ~30 min). The PVDF membrane was sealed with skim milk (5% TBST) and incubated with primary antibody at 4 °C overnight. The secondary antibody coupled with HRP was incubated at room temperature for 1.5 h. The signal was developed by SuperSignal West Femto ECL (Thermo Science™ Emm™) and visualized by Omega Lum C Imaging System (Aplegen, USA).

**In vivo vaccination experiment.** C57BL/6J aged 4–6 weeks mice were procured from Beijing Vital River Laboratory Animal Technology Co., Ltd. The mice were raised in well-ventilated conditions, with a relative humidity of 50–60% at 20 °C. After 10 days of adaptive feeding, the mice were applied for the experiment. This study was performed with the Institutional Animal Care and Use Committee (IACUC) of Sun Yat-Sen University (Approval No: SYSU-IACUC-2021-000818). Animals were treated as the guidelines of IACUC.

The C57BL/6J female mice were randomly separated into 4 groups with each group containing 15 mice. Those 15 mice in each group were further divided into three subgroups (n = 5), then flow cytometry of dendritic cells in lymph nodes, flow cytometry of tumor and spleen lymphocytes, and tumor volume was detected, respectively. Modality-specific details were described below: 1)

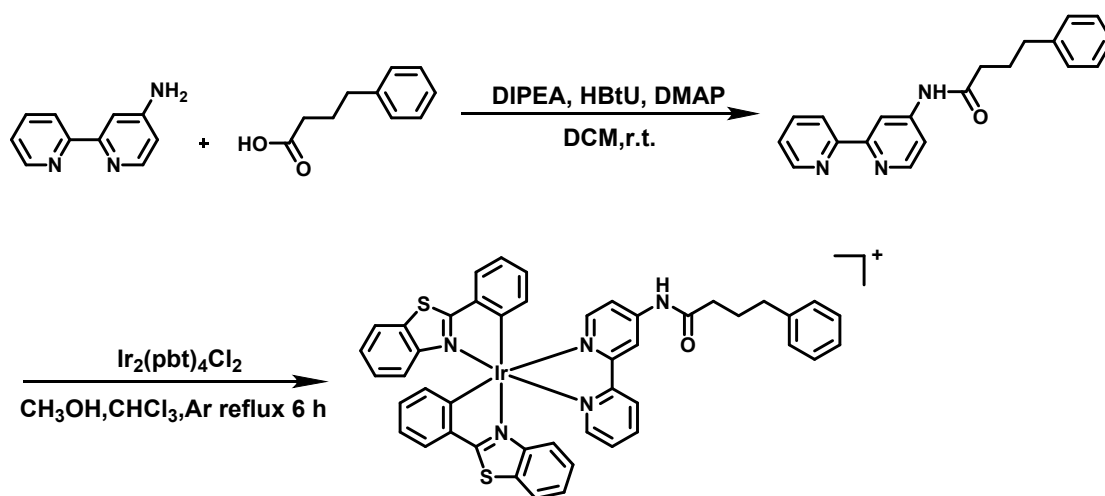
Control group; 2) light only group; 3) Ir-pbt-Bpa only group; 4) Ir-pbt-Bpa + light group.  $2 \times 10^5$  B16F10 cells were suspended in 100  $\mu$ L of a 2:1 mixture of XXXatrigel and subcutaneously injected into the right flanks of C57BL/6J mice. After 6 days (on day 1), when the tumor volume grew to 60 mm<sup>3</sup>, the next experiment was carried out. Mice in Group 1 were left intact without any treatment; mice in Group 2 were irradiated (two-photon 750 nm laser, 50 mW, 5 min); mice in Group 3 were injected intratumorally (3 mg/kg); Group 4 were injected intratumorally (3 mg/kg) respectively, and irradiated 4 h later (two-photon 750 nm laser, 50 mW, 5 min). On day 2,  $2 \times 10^5$  B16F10 cells were suspended and subcutaneously injected into the left flanks of mice in each group. On day 4, the treatments of day 1 were repeated for each group. On day 7, dendritic cells of lymph nodes were extracted from 5 mice in each group for the detection of flow cytometry. On day 12, lymphocytes from the tumors and spleens were detected by flow cytometry from 5 mice in each group. The immunofluorescence antibodies involved mainly included: (1) pacific blue-CD45, percpCy5.5-CD11C, FITC-CD80, PE-CD86; (2) PE-CD3, APC-CD4, SB600 (Q-Dot)-CD8, Percp-Cy5.5-CD44, APC-CY7-CD62L; (3) PE-CY7- CD3, PercpCy5.5-CD4, APC-CD25, PE-Foxp3; (4) FITC-CD8, FITC-Foxp3 (pseudo-red). The tumor volume and weight of mice were measured every two days. Tumor volume (V) was calculated by measuring the length (L) and width (W), and calculated as  $V = L \times W^2 \times 0.5$ . Tumors, spleens, and major organs of mice in each group were fixed with 4% paraformaldehyde and sliced. The slices of the tumor and spleen were stained with immunofluorescence of CD8 and Foxp3, and the heart, liver, spleen, lung, kidney, brain, intestine, and distant tumors were stained with H&E.

**Ethics Statement.** This study was performed with the Institutional Animal Care and Use Committee (IACUC) of Sun Yat-Sen University (Approval No: SYSU-IACUC-2021-000818). Animals were treated as the guidelines of IACUC.

## References

1. G. Li, Y. Chen, J. Wang, J. Wu, G. Gasser, L. Ji and H. Chao, *Biomaterials*, 2015, 63, 128-136.
2. L. Wang, R. Guan, L. Xie, X. Liao, K. Xiong, T. W. Rees, Y. Chen, L. Ji and Chao, H. *Angew.Chem. Int. Ed.*, 2021, 60, 4657-4665.
3. P. Zhang, H. Huang, Y. Chen, J. Wang, L. Ji and H. Chao, *Biomaterials*, 2015, 53, 522-531.
4. C. Xu and W. W. Webb, *JOSA B*, 1996, 13, 481-491.
5. R. Guan, Y. Chen, L. Zeng, T. W. Rees, C. Jin, J. Huang, Z. Chen, L Ji and H. Chao, *Chem. Sci.*, 2018, 9, 5183-5190.

## Supplementary Notes



**Scheme S1.** The synthetic route of Ir-pbt-Bpa.

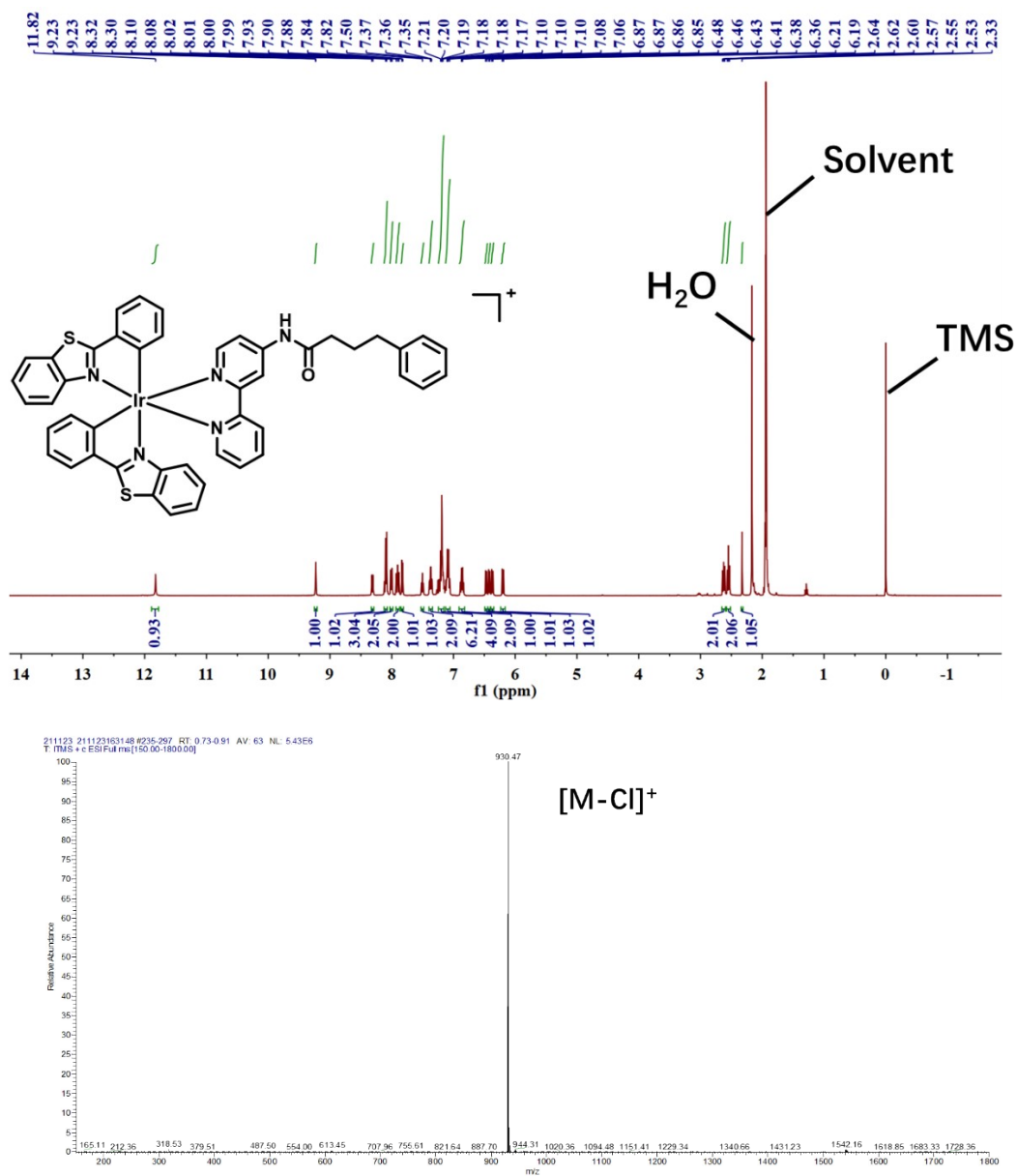


**Fig. S1** <sup>1</sup>H NMR spectrum (400 MHz, CD<sub>3</sub>CN) and ESI-MS spectra of Ir-pbt-Bpa in CH<sub>3</sub>OH.

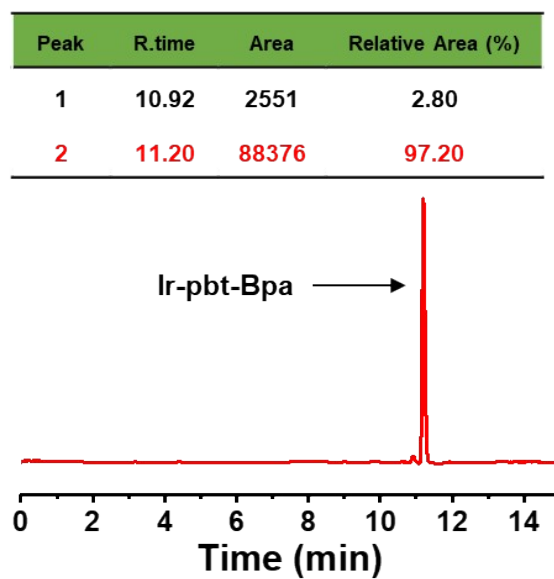


Fig. S2 The purity of Ir-pbt-Bpa was assessed by HPLC.

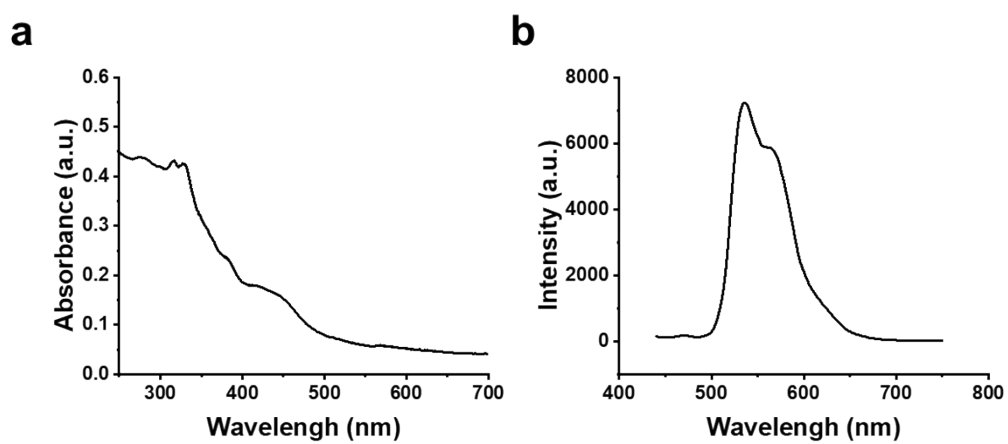
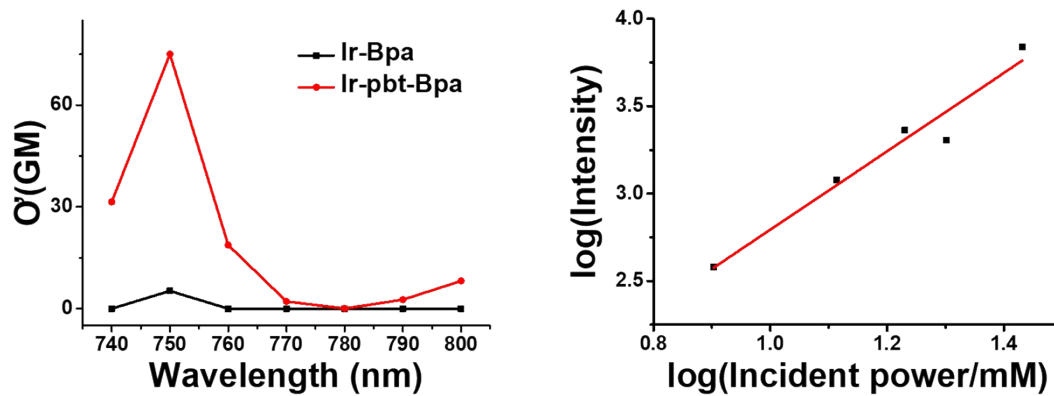
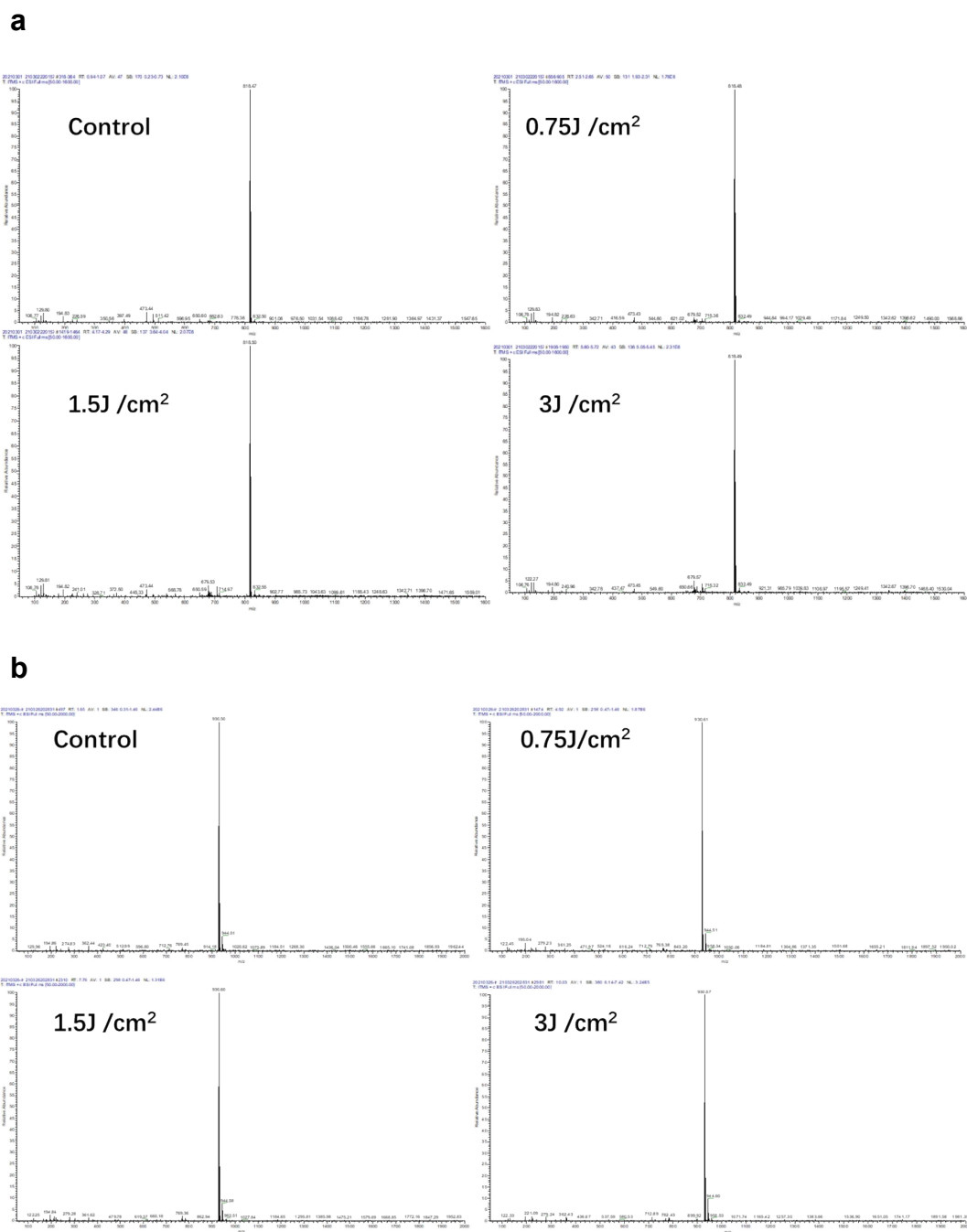


Fig. S3 Photophysical properties of Ir-pbt-Bpa. A) UV/Vis absorption spectrum of Ir-pbt-Bpa in phosphate-buffered saline (10  $\mu$ M) at room temperature. B) Emission spectrum ( $\lambda_{\text{ex}} = 405$  nm) of Ir-pbt-Bpa in phosphate-buffered saline (10  $\mu$ M) at room temperature.



**Fig. S4** Two-photon absorption cross-section spectra of Ir-Bpa and Ir-pbt-Bpa upon excitation from 740-800 nm.



**Fig. S5** Assessment of the photostability of a) Ir-Bpa, b) Ir-pbt-Bpa. The metal complexes were dissolved in water (10  $\mu$ M) and exposed to continuous 405 nm LED irradiation with different power densities (0.75 J/cm<sup>2</sup>, 1.5 J/cm<sup>2</sup>, 3 J/cm<sup>2</sup>). The identity of the compound was analyzed by electrospray ionization mass spectrometry.



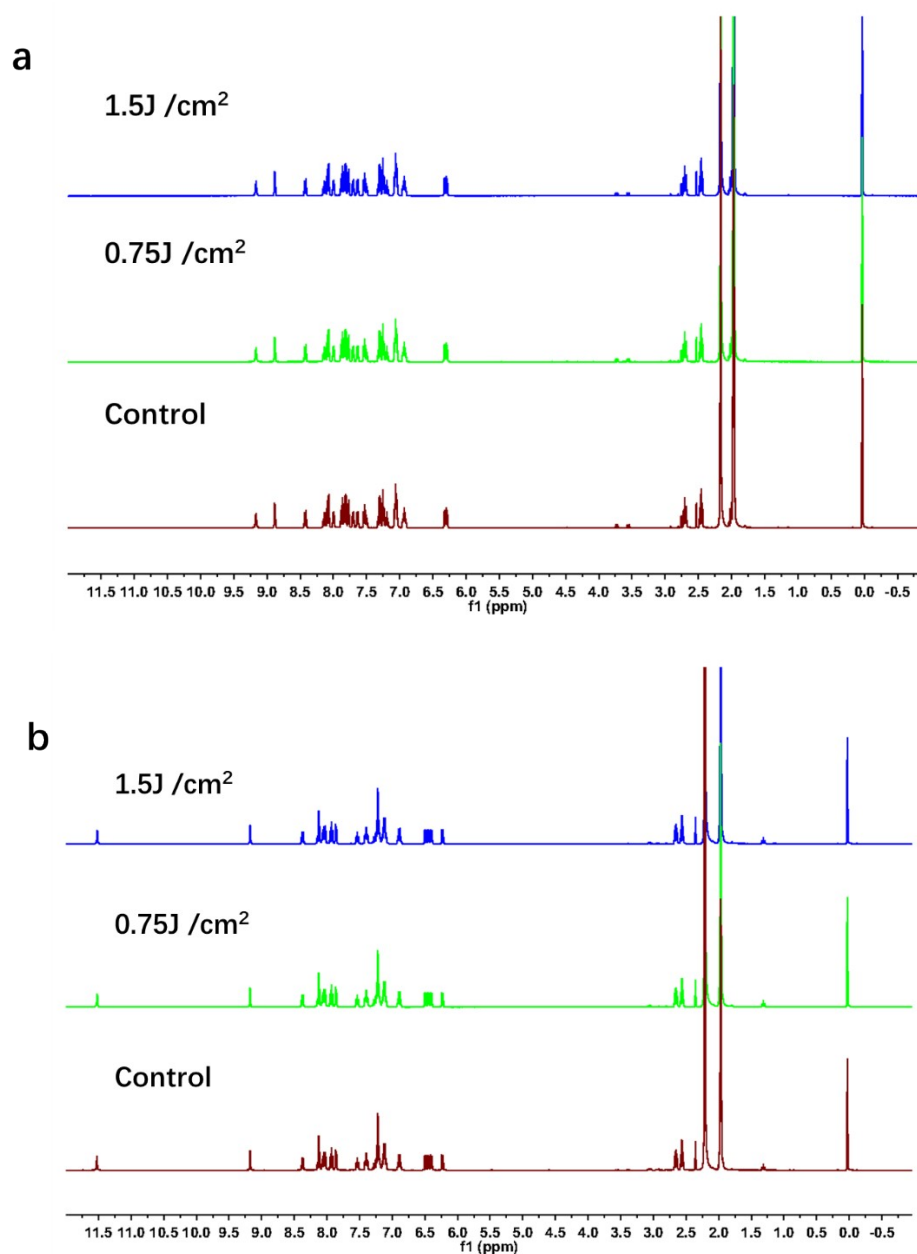


**Fig. S6** Assessment of the photostability of a) Ir-Bpa, b) Ir-pbt-Bpa. The metal complexes were dissolved in CD<sub>3</sub>CN and exposed to continuous 405 nm LED irradiation with different power densities (0.75 J/cm<sup>2</sup>, 1.5 J/cm<sup>2</sup>). The identity of the compound was analyzed by proton nuclear magnetic resonance spectroscopy.

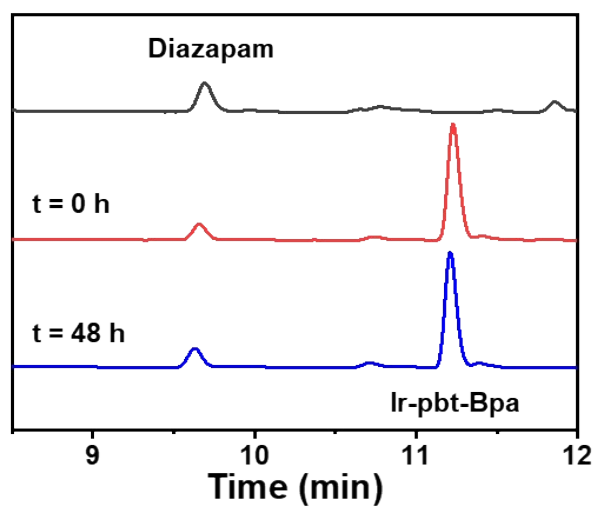


Fig. S7 HPLC analysis of Ir-pbt-Bpa incubated in FBS for 0 h or 48 h.

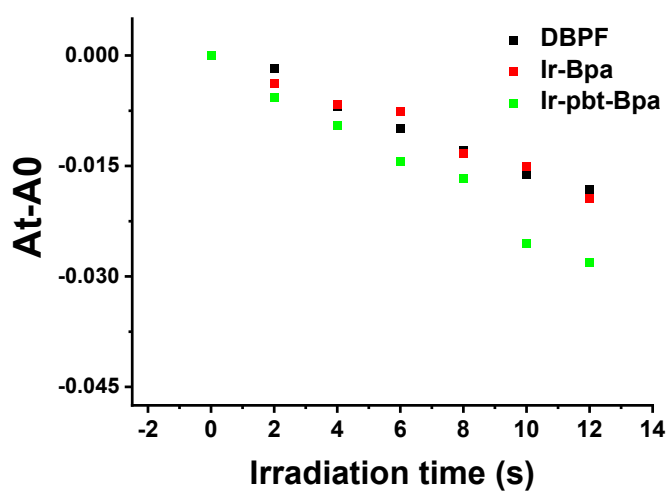
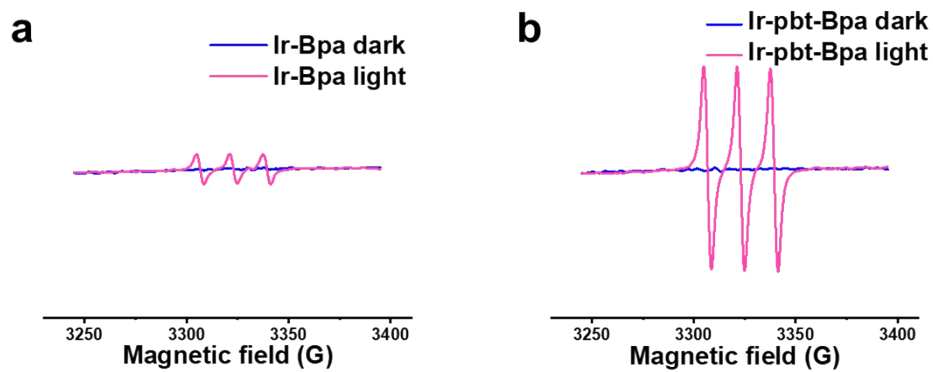
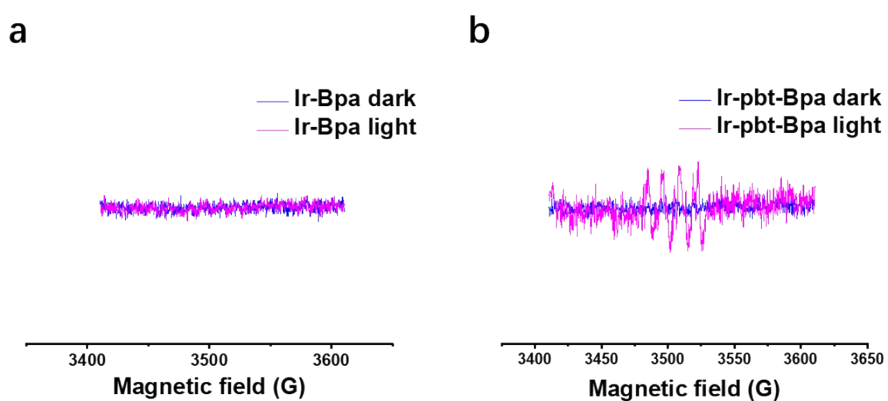


Fig. S8 Determination of the singlet oxygen quantum yield of Ir-Bpa and Ir-pbt-Bpa.  $\lambda_{irr} = 405$  nm.



**Fig. S9** Electron spin resonance spectrum of a) Ir-Bpa and b) Ir-pbt-Bpa upon incubation with the  $^1\text{O}_2$  scavenger 2,2,6,6-tetramethylpiperidine in the dark or upon irradiation ( $\lambda_{\text{irr}} = 405$  nm).



**Fig. S10** Electron spin resonance spectrum of a) Ir-Bpa and b) Ir-pbt-Bpa upon incubation with the  $\bullet\text{O}_2^-$  radical scavenger 5,5-dimethyl-1-pyrroline N-oxide in the dark or upon irradiation ( $\lambda_{\text{irr}} = 405$  nm).

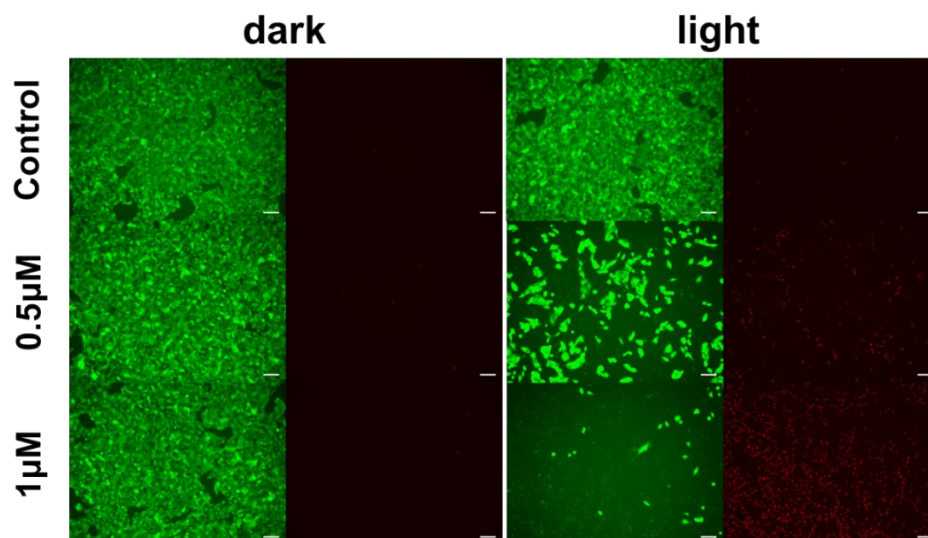


**Fig. S11** Fluorescence microscopy images of B16F10 cells co-stained by calcein-AM (live, green) and propidium iodide (dead, red). B16F10 cells were incubated with Ir-pbt-Bpa (0.5  $\mu$ M, 1  $\mu$ M) for 4 h with/without irradiation (405 nm LED, 0.75 J/cm<sup>2</sup>). Scale bar:100  $\mu$ m.

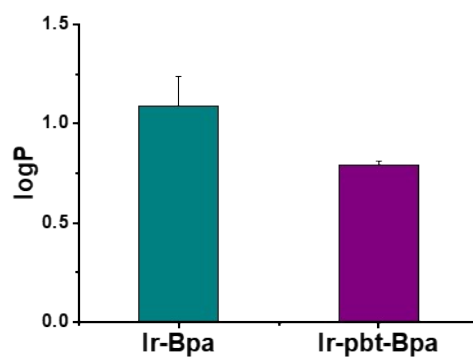


**Fig. S12** Log P values of the complexes Ir-Bpa and Ir-pbt-Bpa.

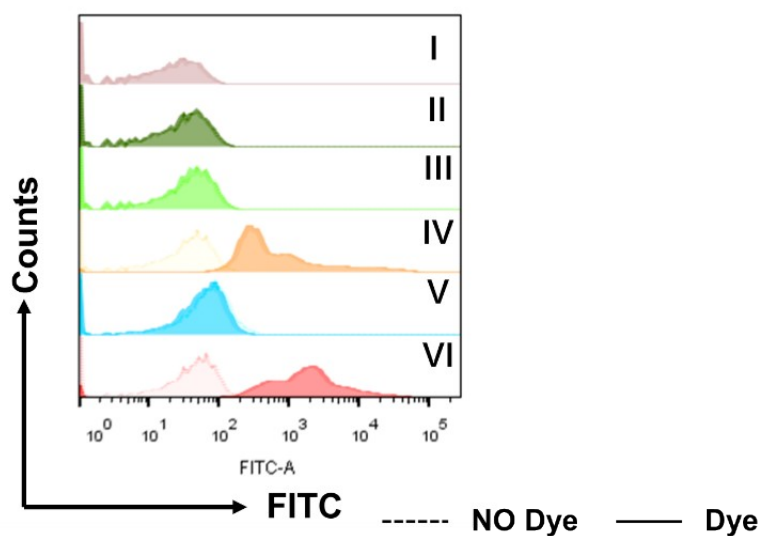


**Fig. S13** Flow cytometry spectrum upon treatment of B16F10 cells with Ir-pbt-Bpa to investigate the ability of the compound to generate ROS. (I): Cells were kept in the dark; (II): Cells were exposed to irradiation (405 nm LED, 0.75 J/cm<sup>2</sup>); (III): Cells were incubated with Ir-pbt-Bpa (Concentration: IC<sub>50</sub> value) for 4 h in the dark, (IV): Cells were incubated with Ir-pbt-Bpa (Concentration: 2xIC<sub>50</sub> value) for 4 h in the dark; (V): Cells were incubated with Ir-pbt-Bpa (Concentration: IC<sub>50</sub> value) for 4 h and exposed to irradiation (405 nm LED, 0.75 J/cm<sup>2</sup>), (VI): Cells were incubated with Ir-pbt-Bpa (Concentration: 2xIC<sub>50</sub> value) for 4 h and exposed to irradiation (405 nm LED, 0.75 J/cm<sup>2</sup>). The dashed lines represent the negative controls without dye.

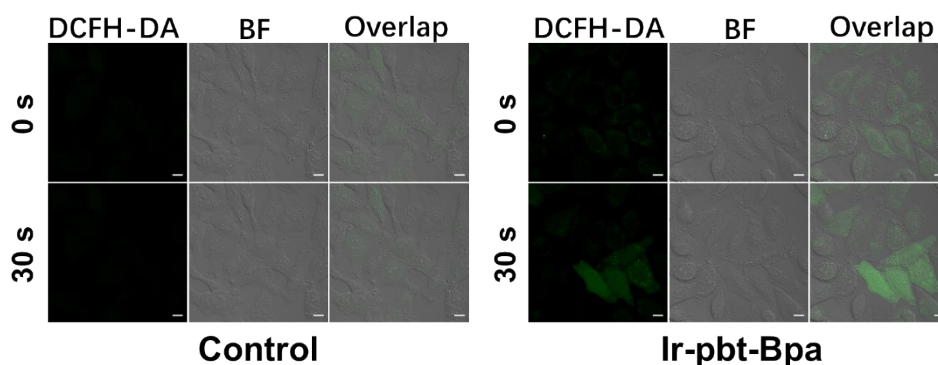


**Fig. S14** Fluorescence microscopy images of ROS of A375 cells upon treatment with Ir-pbt-Bpa (2.5 μM) for 4 h in the dark or upon irradiation (two-photon 750 nm laser). Irradiation: 50 mW/cm<sup>2</sup>, 30 s.

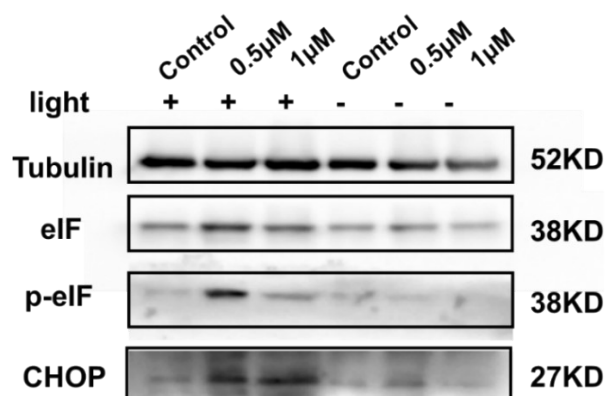


**Fig. S15** Representative immunoblotting images of the Western Blot of B16F10 cells upon treatment with Ir-pbt-Bpa in the dark (-) or upon irradiation (+). Irradiation: 405 nm LED, 0.75 J/cm<sup>2</sup>.

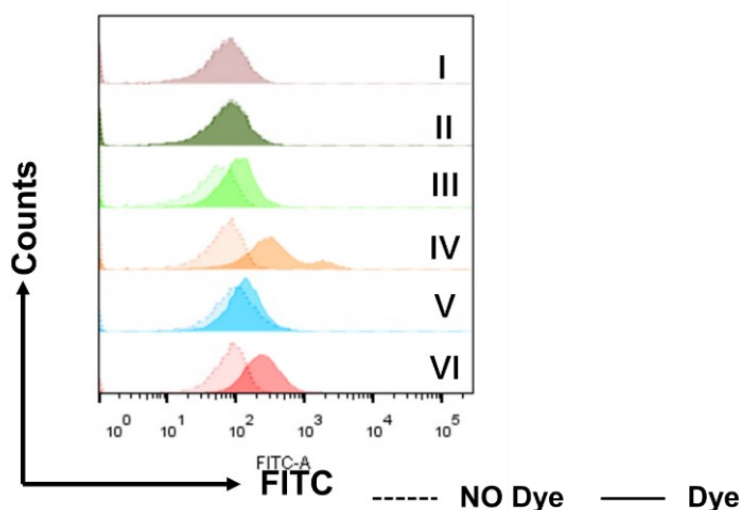


**Fig. S16** Flow cytometry spectrum upon treatment of B16F10 cells with Ir-pbt-Bpa to investigate the ability of the compound to release Ca<sup>2+</sup> ions. (I): Cells were kept in the dark; (II): Cells were exposed to irradiation (405 nm LED, 0.75 J/cm<sup>2</sup>); (III): Cells were incubated with Ir-pbt-Bpa (Concentration: IC<sub>50</sub> value) for 4 h in the dark, (IV): Cells were incubated with Ir-pbt-Bpa (Concentration: 2xIC<sub>50</sub> value) for 4 h in the dark; (V): Cells were incubated with Ir-pbt-Bpa (Concentration: IC<sub>50</sub> value) for 4 h and exposed to irradiation (405 nm LED, 0.75 J/cm<sup>2</sup>), (IV): Cells were incubated with Ir-pbt-Bpa (Concentration: 2xIC<sub>50</sub> value) for 4 h and exposed to irradiation (405 nm LED, 0.75 J/cm<sup>2</sup>). The dashed lines represent the negative controls without dye.

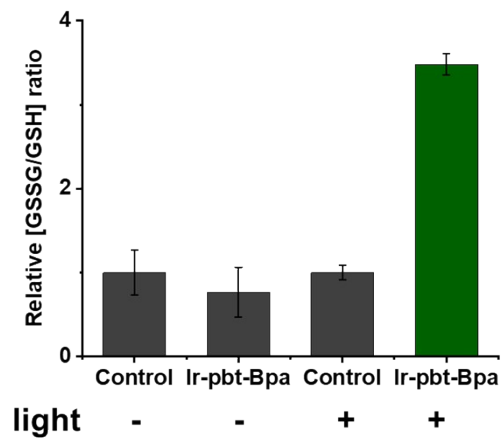


**Fig. S17** Relative glutathione-disulfide/glutathione ratio upon treatment of A375 cells with Ir-pbt-Bpa (1  $\mu$ M) in the dark (-) or upon irradiation (+). Irradiation: 405 nm LED, 0.75 J/cm<sup>2</sup>.

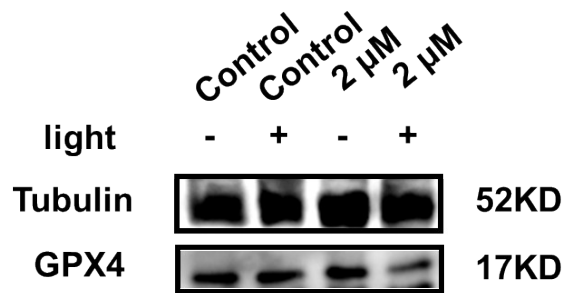


**Fig. S18** Representative immunoblotting images of the Western Blot of A375 cells upon treatment with Ir-pbt-Bpa (2  $\mu$ M) in the dark (-) or upon irradiation (+). Irradiation: 405 nm LED, 0.75 J/cm<sup>2</sup>.

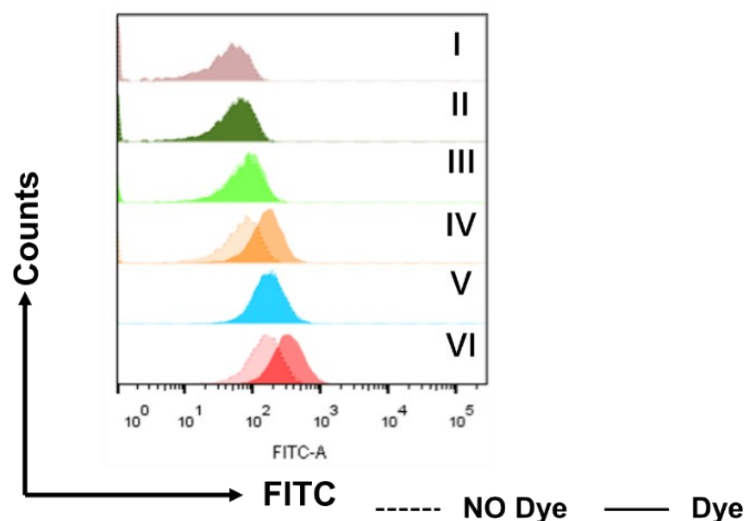


**Fig. S19** Flow cytometry spectrum upon treatment of B16F10 cells with Ir-pbt-Bpa to investigate the ability of the compound to generate LPO. (I): Cells were kept in the dark; (II): Cells were exposed to irradiation (405 nm LED, 0.75 J/cm<sup>2</sup>); (III): Cells were incubated with Ir-pbt-Bpa (Concentration: IC<sub>50</sub> value) for 4 h in the dark, (IV): Cells were incubated with Ir-pbt-Bpa (Concentration: 2xIC<sub>50</sub> value) for 4 h in the dark; (V): Cells were incubated with Ir-pbt-Bpa (Concentration: IC<sub>50</sub> value) for 4 h and exposed to irradiation (405 nm LED, 0.75 J/cm<sup>2</sup>), (VI): Cells were incubated with Ir-pbt-Bpa (Concentration: 2xIC<sub>50</sub> value) for 4 h and exposed to irradiation (405 nm LED, 0.75 J/cm<sup>2</sup>). The dashed lines represent the negative controls without dye.

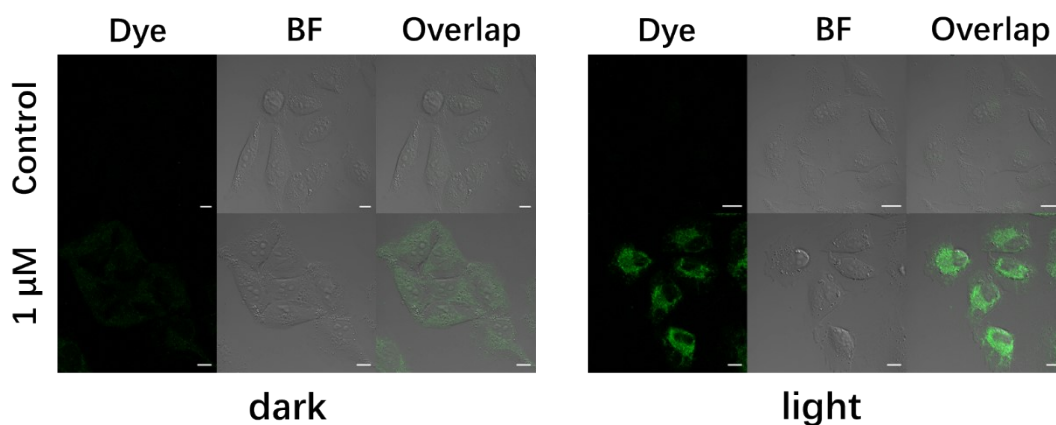


**Fig. S20** Confocal laser scanning microscopy images of A375 cells upon incubation with Ir-pbt-Bpa for 4 h and LPO-specific dye in the dark or upon irradiation (405 nm LED, 0.75 J/cm<sup>2</sup>).



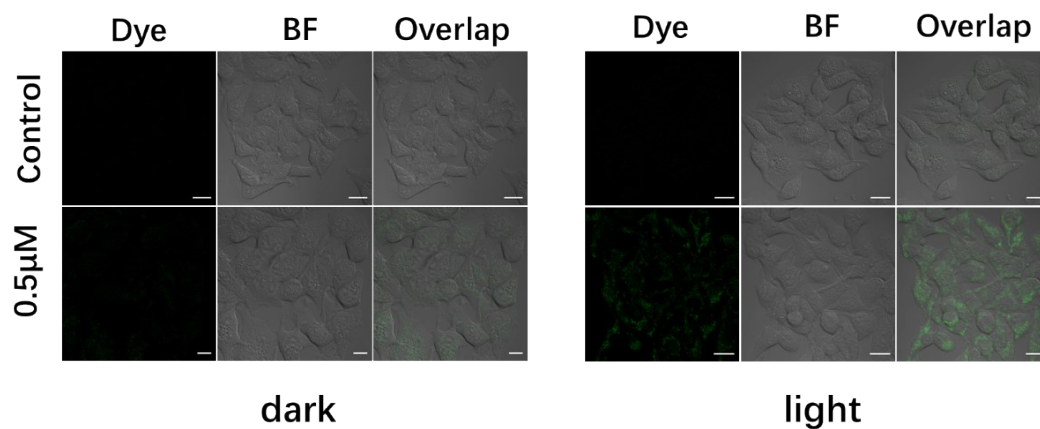


**Fig. S21** Confocal laser scanning microscopy images of B16F10 cells upon incubation with Ir-pbt-Bpa for 4 h and LPO-specific dye in the dark or upon irradiation (405 nm LED, 0.75 J/cm<sup>2</sup>).

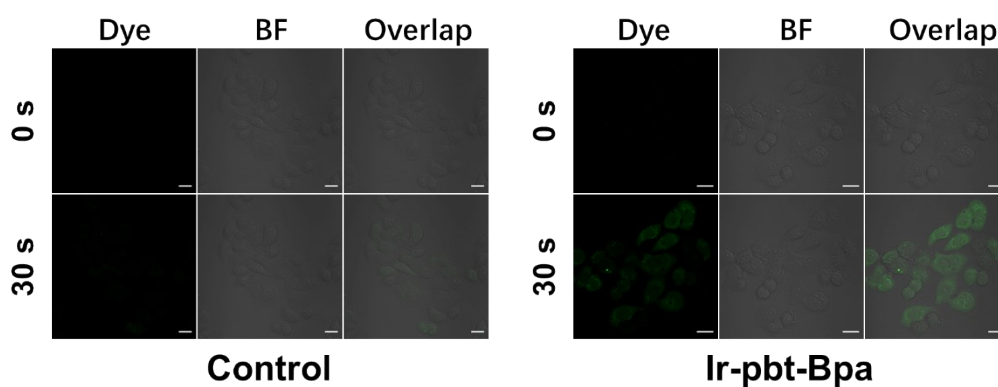


**Fig. S22** Fluorescence microscopy images of LPO of A375 cells upon treatment with Ir-pbt-Bpa (2.5 µM) for 4 h in the dark or upon irradiation (two-photon 750 nm laser). Irradiation: 50 mW/cm<sup>2</sup>, 30 s.

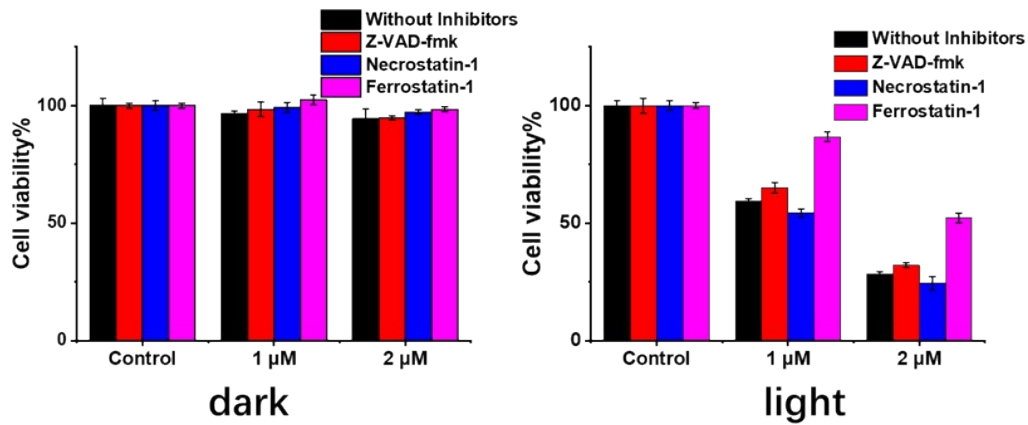


**Fig. S23** Cell viability of A375 cells upon pre-incubation with the cell death inhibitors. The cells were preincubated with Z-VAD-fmk (10  $\mu$ M), 3-methyladenine (100  $\mu$ M), Ferrostatin-1 (10  $\mu$ M), or Necrostatin-1 (60  $\mu$ M) for 30 min. The cells were incubated with various concentrations of Ir-pbt-Bpa for 4 h. Medium containing Ir-pbt-Bpa was replaced with the corresponding fresh culture medium with or without the corresponding inhibitors. And then kept in the dark or exposed to light irradiation (405 nm LED, 0.75 J/cm<sup>2</sup>). After an additional 20 h incubation, the cell viability was assessed using an MTT assay.

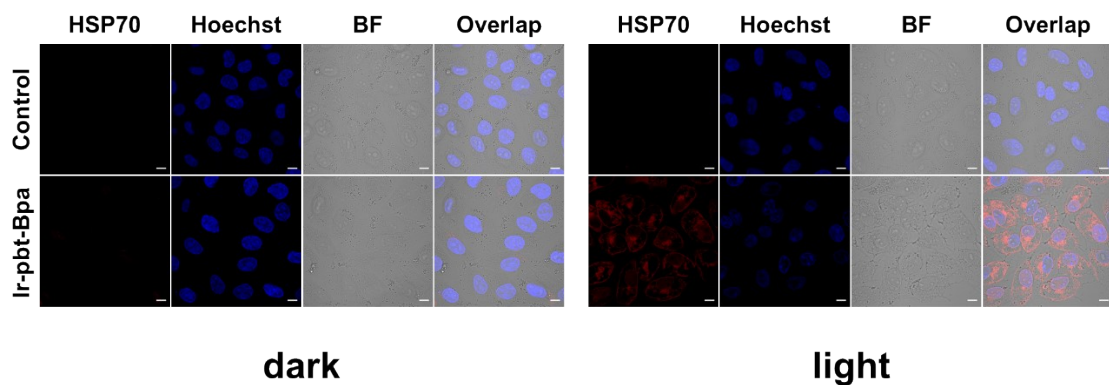


**Fig. S24** Immunofluorescence confocal laser scanning microscopy upon treatment of A375 cells with Ir-pbt-Bpa (1  $\mu$ M) for HSP70. Light irradiation: 405 nm LED, 0.75 J/cm<sup>2</sup>.

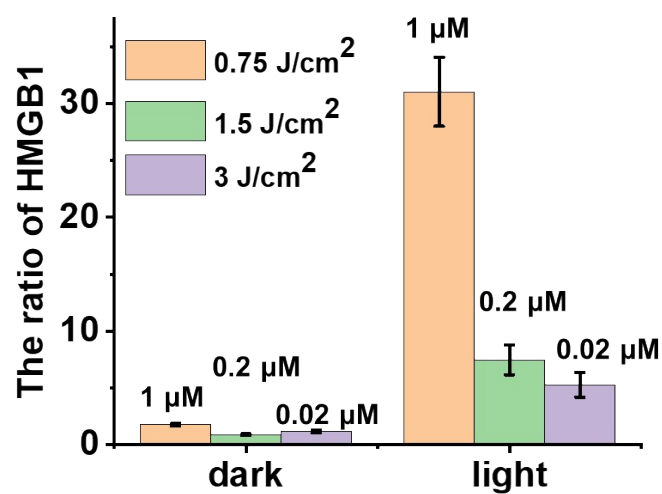


**Fig. S25** Release of nuclear high-mobility group box 1 protein into the cell culture supernatant upon treatment of A375 cells with Ir-pbt-Bpa (1 μM, 0.2 μM, 0.02 μM) for 4 h. The cells were kept in the dark or exposed to irradiation (405 nm LED, 0.75 J/cm<sup>2</sup>, 1.5 J/cm<sup>2</sup>, 3 J/cm<sup>2</sup>).

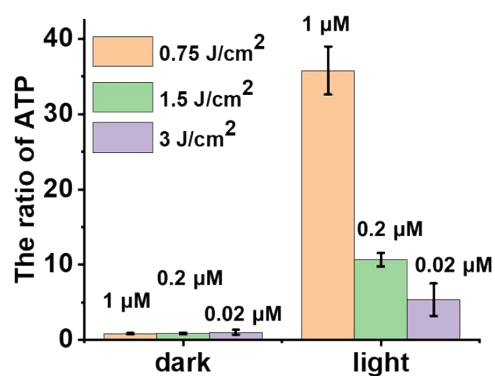


**Fig. S26** Release of adenosine triphosphate into the cell culture supernatant upon treatment of A375 cells with Ir-pbt-Bpa (1 μM, 0.2 μM, 0.02 μM) for 4 h. The cells were kept in the dark or exposed to irradiation (405 nm LED, 0.75 J/cm<sup>2</sup>, 1.5 J/cm<sup>2</sup>, 3 J/cm<sup>2</sup>).

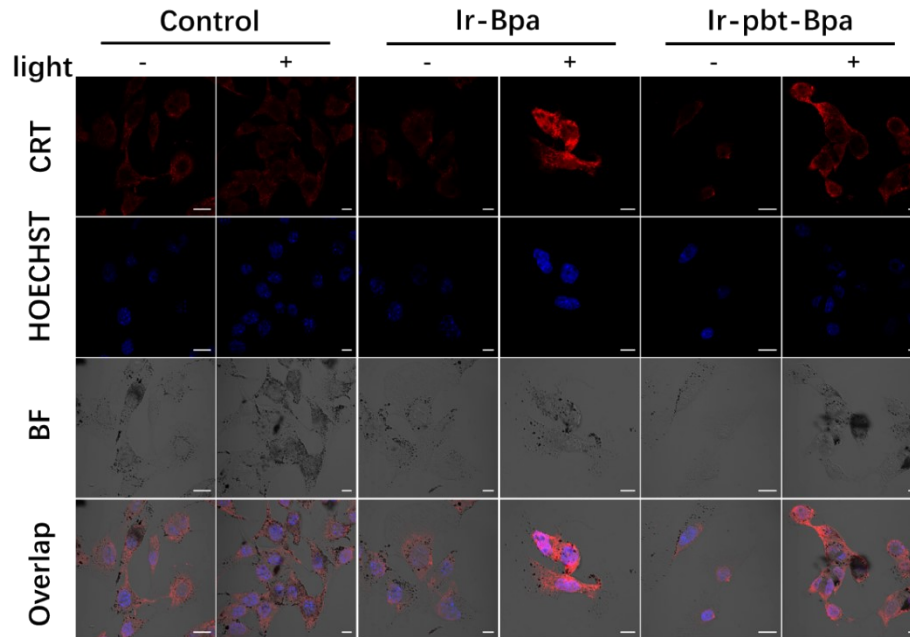


**Fig. S27** Immunofluorescence confocal laser scanning microscopy upon treatment of B16F10 cells with Ir-Bpa and Ir-pbt-Bpa (0.5  $\mu$ M) for 4 h. The cells were kept in the dark or exposed to irradiation (405 nm LED, 0.75 J/cm<sup>2</sup>). The cells were further stained with a calreticulin-specific antibody. Scale bar: 10  $\mu$ m.

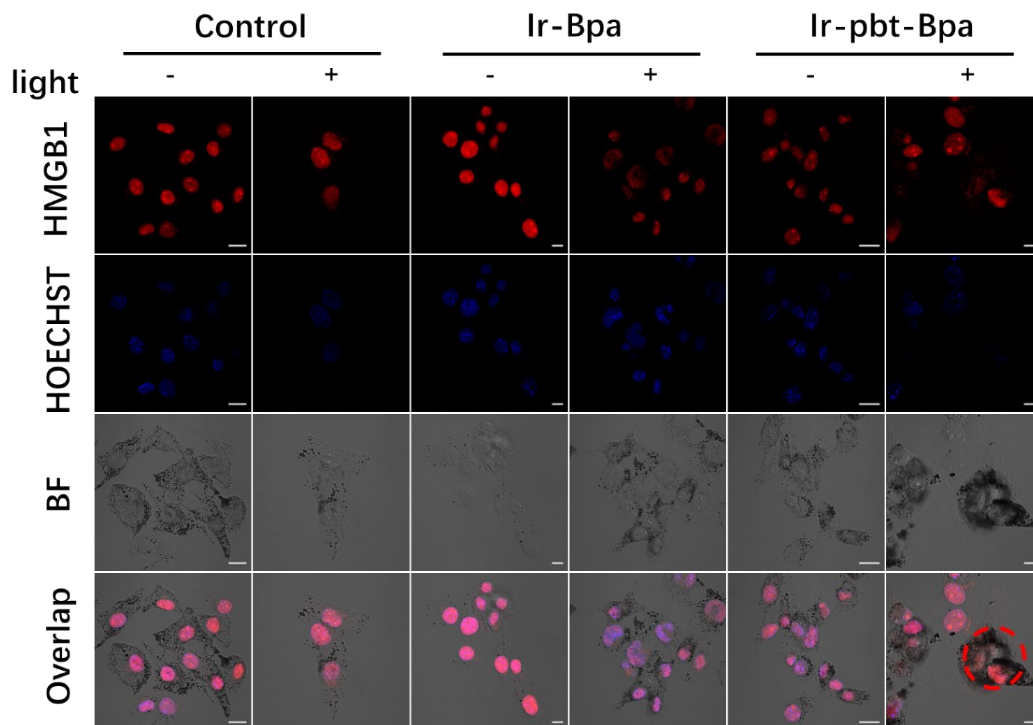


**Fig. S28** Immunofluorescence confocal laser scanning microscopy upon treatment of B16F10 cells with Ir-Bpa and Ir-pbt-Bpa (0.5  $\mu$ M) for 4 h. The cells were kept in the dark or exposed to irradiation (405 nm LED, 0.75 J/cm<sup>2</sup>). The cells were further stained with a nuclear high-mobility group box 1 protein-specific antibody. Scale bar: 10  $\mu$ m.

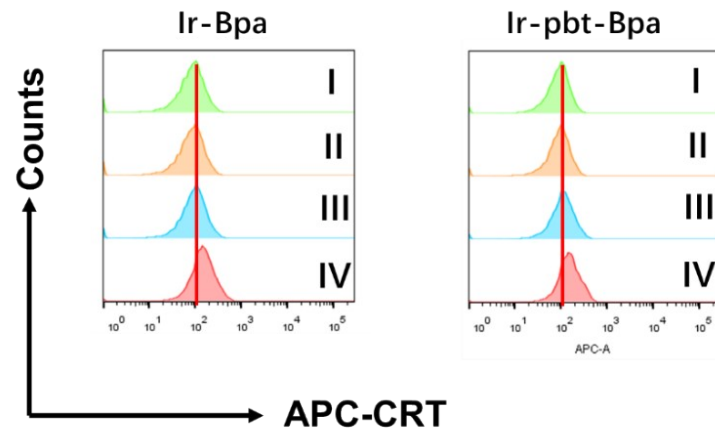


**Fig. S29** Flow cytometry spectrum to investigate the translocation of calreticulin upon treatment of B16F10 cells with Ir-Bpa and Ir-pbt-Bpa (0.5  $\mu$ M) for 4 h. (I): Cells were kept in the dark; (II): Cells were exposed to irradiation (405 nm LED, 0.75 J/cm<sup>2</sup>); (III): Cells were incubated with the compound for 4 h in the dark, (IV): Cells were incubated with the compound for 4 h and exposed to irradiation (405 nm LED, 0.75 J/cm<sup>2</sup>).

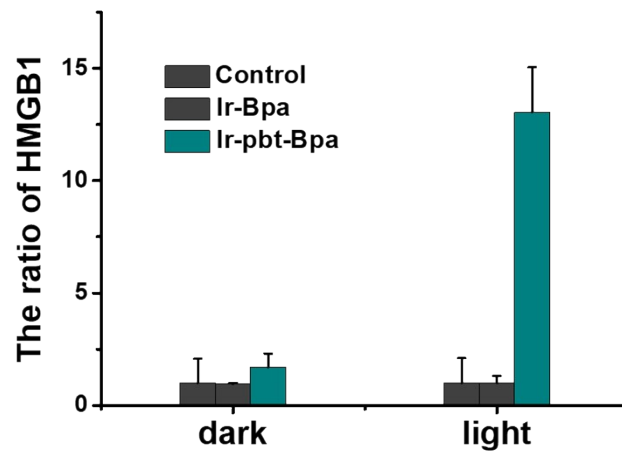


**Fig. S30** Release of nuclear high-mobility group box 1 protein into the cell culture supernatant upon treatment of B16F10 cells with Ir-Bpa and Ir-pbt-Bpa (0.5  $\mu$ M) for 4 h. The cells were kept in the dark or exposed to irradiation (405 nm LED, 0.75 J/cm<sup>2</sup>).

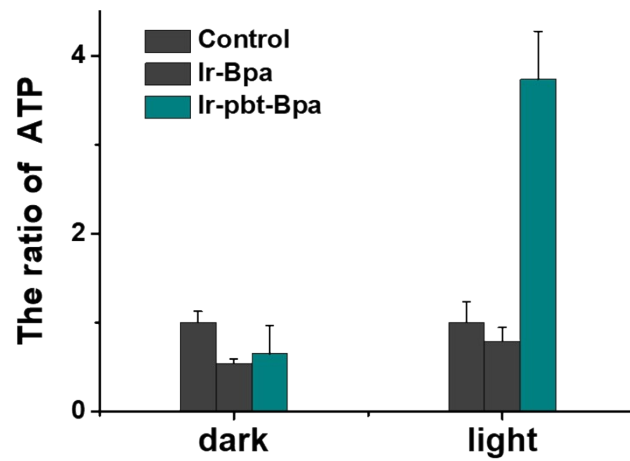


**Fig. S31** Release of adenosine triphosphate into the cell culture supernatant upon treatment of B16F10 cells with Ir-Bpa and Ir-pbt-Bpa ( $0.5 \mu\text{M}$ ) for 4 h. The cells were kept in the dark or exposed to irradiation (405 nm LED,  $0.75 \text{ J}/\text{cm}^2$ ).

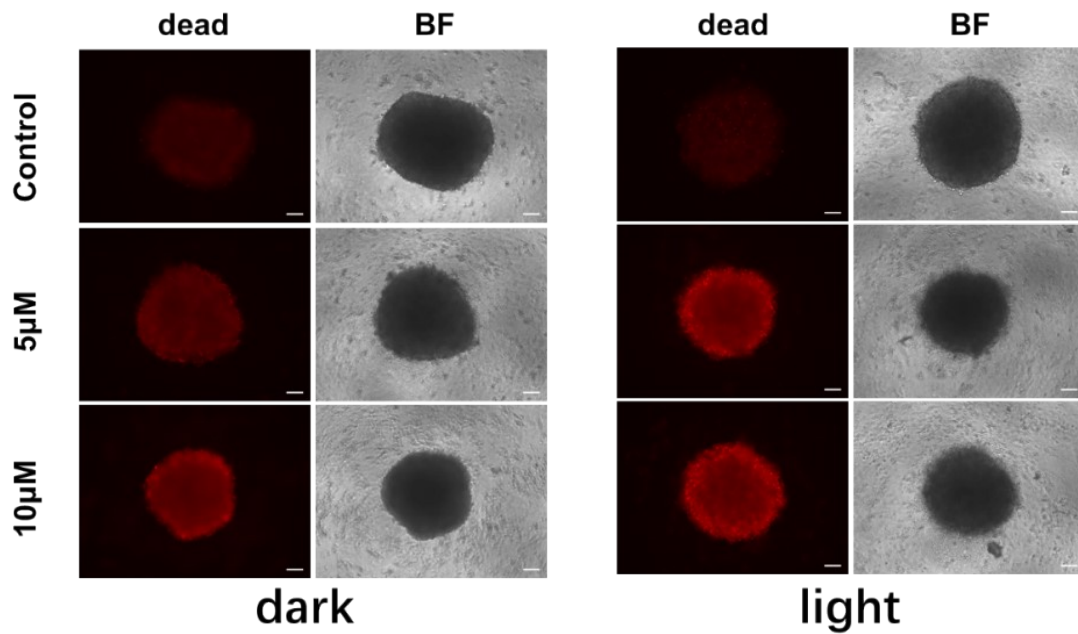


**Fig. S32** Fluorescence microscopy images of A375 MCTS co-stained by propidium iodide (dead, red). A375 MCTS were incubated with Ir-pbt-Bpa ( $5 \mu\text{M}$ ,  $10 \mu\text{M}$ ) for 12 h with/without irradiation (750 nm Laser, 50 mW, 5 min). Scale bar:  $100 \mu\text{m}$ .

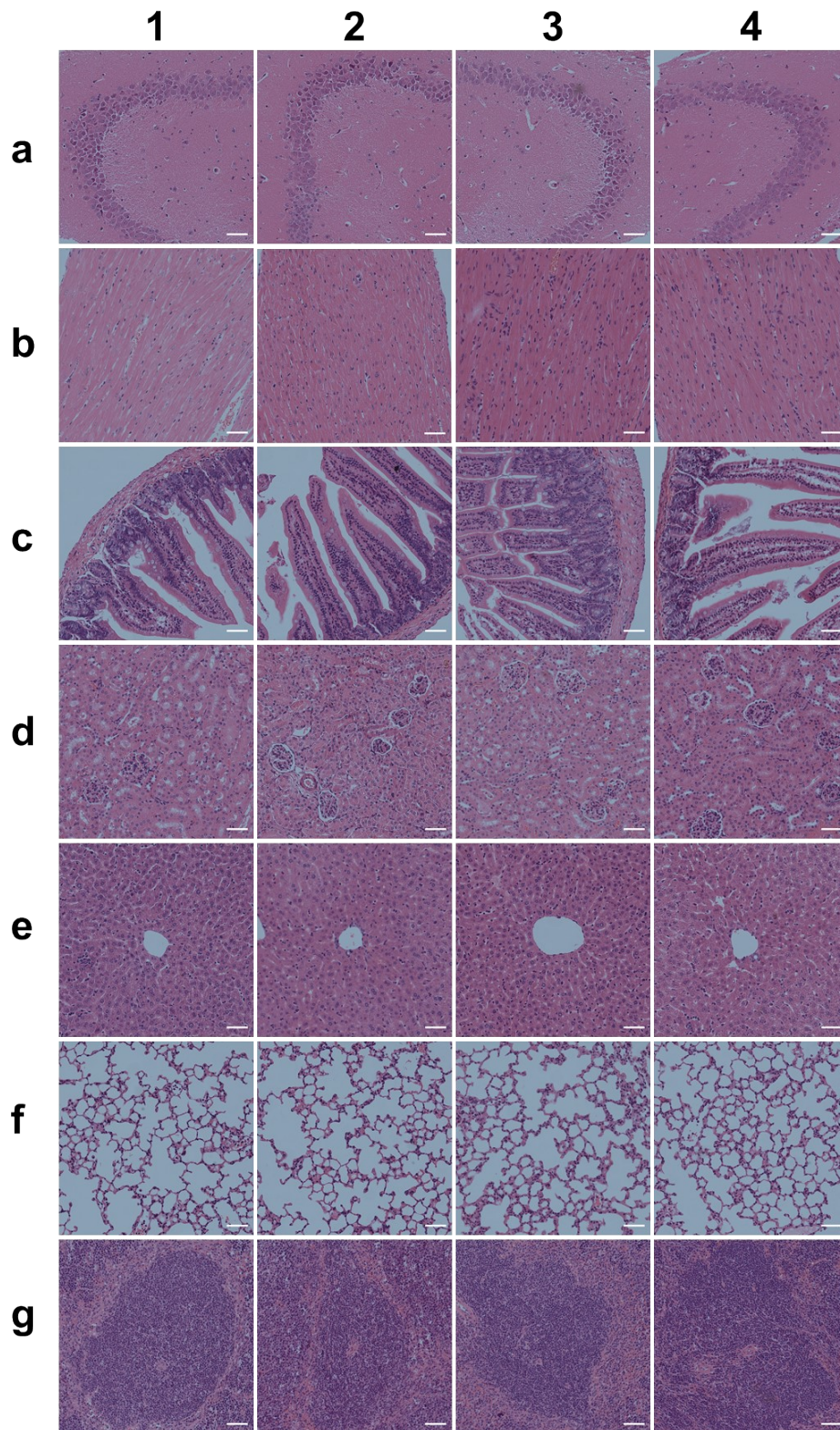


**Fig. S33** Histological examination of the main organs of the mice on day 12. A: brain; b: heart; c: intestine; d kidney; e liver; f: lung; g: spleen. Sections for light microscope stained by hematoxylin-eosin (H&E). Scale bar: 50  $\mu$ m.

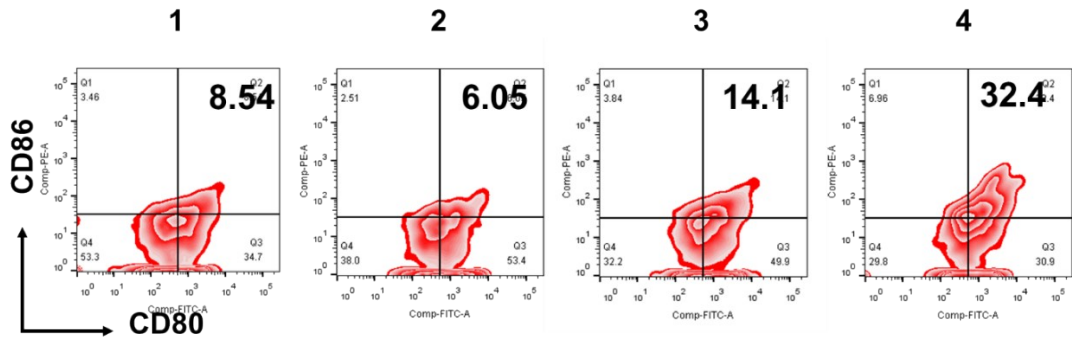


**Fig. S34** Representative flow cytometry plots indicate the proportions of dendritic cells in lymph nodes on day 7. 1) Control; 2) light only; 3) Ir-pbt-Bpa only; 4) Ir-pbt-Bpa + light.

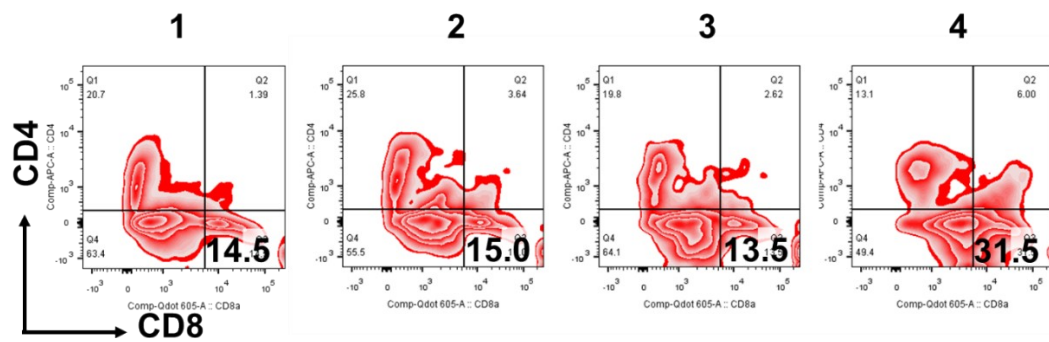


**Fig. S35** Representative flow cytometry plots indicate the proportions of CD8<sup>+</sup> T cells in tumors on day 12. 1) Control; 2) light only; 3) Ir-pbt-Bpa only; 4) Ir-pbt-Bpa + light.

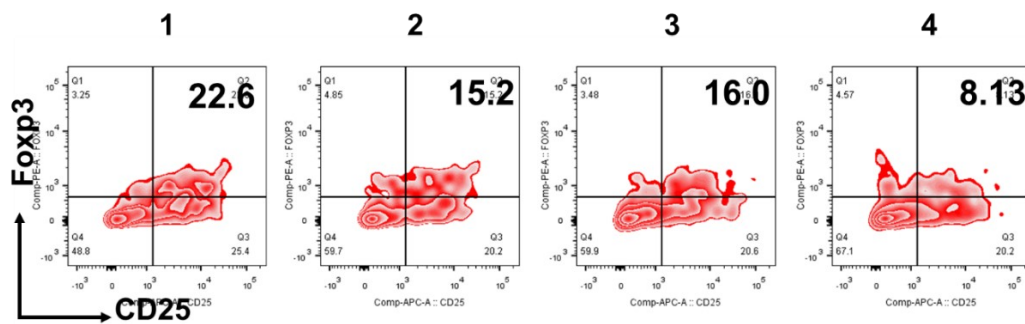


**Fig. S36** Representative flow cytometry plots indicate the proportions of regulatory T cells in tumors on day 12. 1) Control; 2) light only; 3) Ir-pbt-Bpa only; 4) Ir-pbt-Bpa + light.



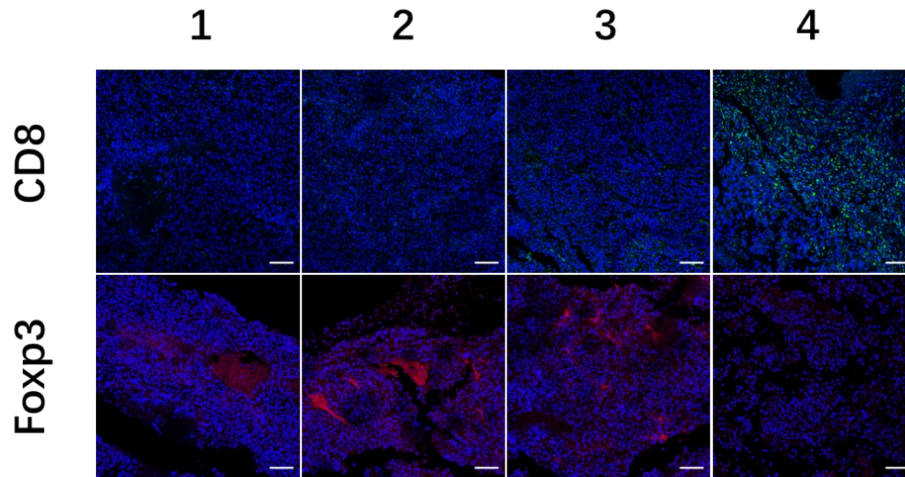


**Fig. S37** Immunofluorescence confocal laser scanning microscopy stained with CD8<sup>+</sup> and Foxp3<sup>+</sup> specific antibodies in secondary tumor slices on day 12. Blue, Hoechst; green, CD8<sup>+</sup> T cells; red, Foxp3<sup>+</sup> T cells; Scale bar: 100  $\mu$ m.

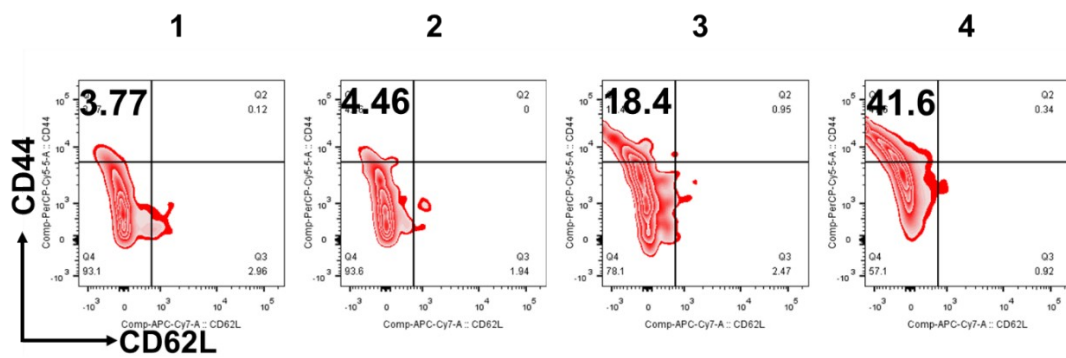


**Fig. S38** Representative flow cytometry plots indicate the proportions of effector memory T cells in tumors on day 12. 1) Control; 2) light only; 3) Ir-pbt-Bpa only; 4) Ir-pbt-Bpa + light.

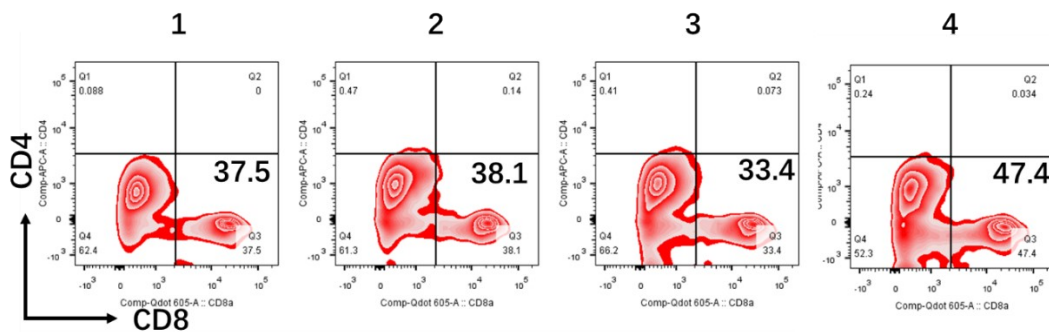


**Fig. S39** Representative flow cytometry plots indicate the proportions of CD8<sup>+</sup> T cells in the spleen on day 12. 1) Control; 2) light only; 3) Ir-pbt-Bpa only; 4) Ir-pbt-Bpa + light.

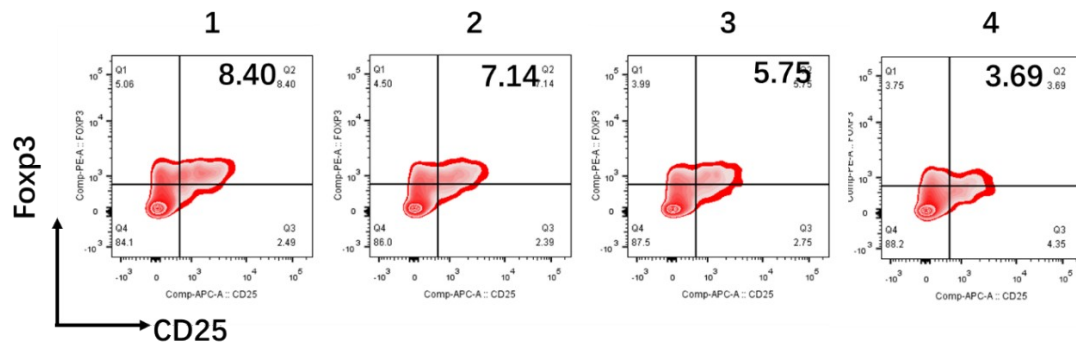


**Fig. S40** Representative flow cytometry plots indicate the proportions of regulatory T cells in spleens on day 12. 1) Control; 2) light only; 3) Ir-pbt-Bpa only; 4) Ir-pbt-Bpa + light.

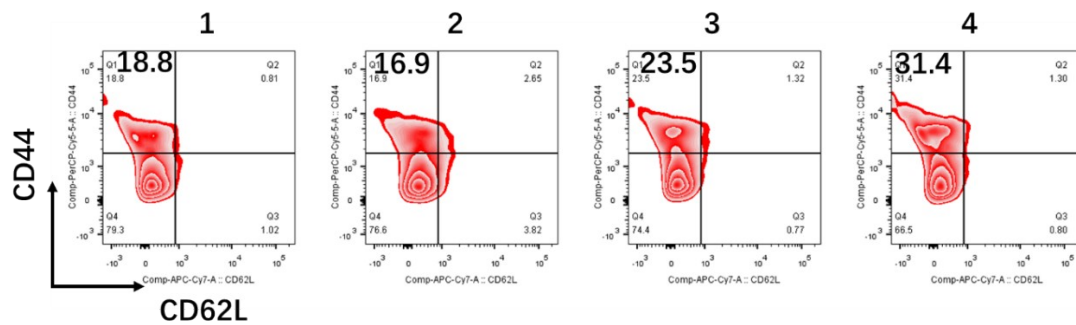


**Fig. S41** Representative flow cytometry plots indicate the proportions of effector memory T cells in the spleen on day 12. 1) Control; 2) light only; 3) Ir-pbt-Bpa only; 4) Ir-pbt-Bpa + light.

**Table S1.** 48 h (photo-)cytotoxicity profile in different cell lines<sup>[a]</sup> (IC<sub>50</sub>, μM).

Cells	Complexes	light <sup>[b]</sup>	dark	PI
A549	Ir-Bpa	1.50 ± 0.18	8.96 ± 0.63	5.93
	Ir-pbt-Bpa	0.39 ± 0.02	15.64 ± 1.40	40.10
LLC	Ir-Bpa	1.36 ± 0.93	14.7 ± 2.77	10.81
	Ir-pbt-Bpa	1.18 ± 0.01	3.19 ± 0.27	2.70
A375	Ir-Bpa	5.00 ± 0.08	6.85 ± 0.33	1.37
	Ir-pbt-Bpa	0.93 ± 0.09	10.87 ± 0.50	11.69
B16F10	Ir-Bpa	2.90 ± 0.82	9.69 ± 0.36	3.34
	Ir-pbt-Bpa	0.42 ± 0.05	14.14 ± 0.55	33.66
MDA-MB-231	Ir-Bpa	1.00 ± 0.71	6.69 ± 0.94	6.69
	Ir-pbt-Bpa	0.53 ± 0.10	9.58 ± 0.36	18.08
4T1	Ir-Bpa	3.98 ± 0.16	8.34 ± 0.14	2.10
	Ir-pbt-Bpa	0.47 ± 0.03	16.30 ± 1.62	34.00
SW620	Ir-Bpa	2.23 ± 0.69	8.21 ± 0.77	3.68
	Ir-pbt-Bpa	1.53 ± 0.26	10.06 ± 1.52	6.58
CT-26	Ir-Bpa	16.76 ± 2.17	15.24 ± 0.18	0.91
	Ir-pbt-Bpa	1.39 ± 0.03	21.99 ± 0.18	15.82

[a] IC<sub>50</sub> values are drug concentrations necessary for 50% inhibition of cell viability. Data are presented as mean ± standard deviations (SD) and cell viability is assessed after 48 h of incubation.

[b] Irradiated by 405 nm LED at 0.75 J/cm<sup>2</sup>.

**Table S2.** (Photo)cytotoxicity profile under various light conditions towards A375 cells (IC<sub>50</sub>, μM).<sup>[a]</sup>

Complex	light <sup>[b]</sup>	PI	light <sup>[c]</sup>	PI	dark
Ir-pbt-Bpa	0.18 ± 0.12	61.99	0.02 ± 0.008	632.17	10.87 ± 0.50

[a] The incubation time is 48 h.

[b] Irradiated by 405 nm LED at 1.5 J/cm<sup>2</sup>.

[c] Irradiated by 405 nm LED at 3 J/cm<sup>2</sup>.

**Table S3.** (Photo)cytotoxicity of Ir-pbt-Bpa towards A375 MCTS (IC<sub>50</sub>, μM).<sup>[a]</sup>

Complex	light <sup>[a]</sup>	dark	PI
Ir-pbt-Bpa	4.90 ± 1.45	25.78 ± 3.22	5.26

[a] The incubation time is 48 h.

[b] Irradiated by two-photon laser at 750 nm (5 min, 50 mW).